Division of Pharmaceutical Technology
Faculty of Pharmacy
University of Helsinki
Finland

Mesoporous silica- and silicon-based materials as carriers for poorly water soluble drugs

Tarja Limnell

ACADEMIC DISSERTATION

To be presented, with the permission of the Faculty of Pharmacy of the University of Helsinki, for public examination in lecture room 1041, Viikki Biocenter 2, on 15th October 2011, at 12 noon.

Helsinki 2011

Supervisors: Professor Jouni Hirvonen
Division of Pharmaceutical Technology
Faculty of Pharmacy
University of Helsinki
Finland

Docent Ann Marie Kaukonen
Division of Pharmaceutical Technology
Faculty of Pharmacy
University of Helsinki
Finland

Docent Hélder A. Santos
Division of Pharmaceutical Technology
Faculty of Pharmacy
University of Helsinki
Finland

Reviewers:

Professor Kristiina Järvinen
School of Pharmacy
Faculty of Health Sciences
University of Eastern Finland
Finland

Professor Niklas Sandler
Pharmaceutical Sciences
Department of Biosciences
Åbo Akademi University
Finland

Opponent:

Professor Carla Caramella
Department of Pharmaceutical Chemistry
Faculty of Pharmacy
University of Pavia
Italy

ISBN 978-952-10-7153-9 (paperback)
ISBN 978-952-10-7154-6 (pdf, http://ethesis.helsinki.fi)
ISSN 1799-7372

Unigrafia
Helsinki, Finland 2011

Abstract

New chemical entities with unfavorable water solubility properties are continuously emerging in drug discovery. Without pharmaceutical manipulations inefficient concentrations of these drugs in the systemic circulation are probable. Typically, in order to be absorbed from the gastrointestinal tract, the drug has to be dissolved. Several methods have been developed to improve the dissolution of poorly soluble drugs.

In this study, the applicability of different types of mesoporous (pore diameters between 2 and 50 nm) silicon- and silica-based materials as pharmaceutical carriers for poorly water soluble drugs was evaluated. Thermally oxidized and carbonized mesoporous silicon materials, ordered mesoporous silicas MCM-41 and SBA-15, and non-treated mesoporous silicon and silica gel were assessed in the experiments. The characteristic properties of these materials are the narrow pore diameters and the large surface areas up to over 900 m^2/g. Loading of poorly water soluble drugs into these pores restricts their crystallization, and thus, improves drug dissolution from the materials as compared to the bulk drug molecules. In addition, the wide surface area provides possibilities for interactions between the loaded substance and the carrier particle, allowing the stabilization of the system. Ibuprofen, indomethacin and furosemide were selected as poorly soluble model drugs in this study. Their solubilities are strongly pH-dependent and the poorest (<100 µg/ml) at low pH values.

The pharmaceutical performance of the studied materials was evaluated by several methods. In this work, drug loading was performed successfully using rotavapor and fluid bed equipment in a larger scale and in a more efficient manner than with the commonly used immersion methods. It was shown that several carrier particle properties, in particular the pore diameter, affect the loading efficiency (typically ~25-40 w-%) and the release rate of the drug from the mesoporous carriers. A wide pore diameter provided easier loading and faster release of the drug. The ordering and length of the pores also affected the efficiency of the drug diffusion. However, these properties can also compensate the effects of each other. The surface treatment of porous silicon was important in stabilizing the system, as the non-treated mesoporous silicon was easily oxidized at room temperature. Different surface chemical treatments changed the hydrophilicity of the porous silicon materials and also the potential interactions between the loaded drug and the particle, which further affected the drug release properties. In all of the studies, it was demonstrated that loading into mesoporous silicon and silica materials improved the dissolution of the poorly soluble drugs as compared to the corresponding bulk compounds (*e.g.* after 30 min ~2-7 times more drug was dissolved depending on the materials). The release profile of the loaded substances remained similar also after 3 months of storage at 30°C/56% RH. The thermally carbonized mesoporous silicon did not compromise the Caco-2 monolayer integrity in the permeation studies and improved drug permeability was observed. The loaded mesoporous silica materials were also successfully compressed into tablets without compromising their characteristic structural and drug releasing properties.

The results of this research indicated that mesoporous silicon/silica-based materials are promising materials to improve the dissolution of poorly water soluble drugs. Their feasibility in pharmaceutical laboratory scale processes was also confirmed in this thesis.

Acknowledgements

This study was carried out at the Division of Pharmaceutical Technology and Drug Discovery and Development Technology Center (currently Centre for Drug Research), Faculty of Pharmacy, University of Helsinki.

I wish to express my gratitude to my supervisor, Professor Jouni Hirvonen for picking my application for a postgraduate position in his group and providing me with excellent research environment for these studies. It was not just once or twice that I left the meetings full of enthusiasm for the future due to his endless positive attitude. My warm thanks belong to Docent Ann Marie Kaukonen for her intensive and caring supervision during the first years of my studies. Docent Hélder A. Santos is greatly acknowledged for his valuable comments and guidance during the final years of this research.

All of my several co-authors deserve sincere thanks for sharing their knowledge with me. Without you all this multidisciplinary research would not have been possible. I would like to thank especially Professor Vesa-Pekka Lehto, Docent Jarno Salonen, Docent Leena Peltonen, Docent Timo Laaksonen, Doctor Leena Laitinen, M.Sc. Teemu Heikkilä and M.Sc. Ermei Mäkilä for sharing their ideas and expertise in favor of this research.

Professor Kristiina Järvinen and Professor Niklas Sandler are acknowledged for carefully reviewing this dissertation manuscript and for providing valuable comments and suggestions for its improvement.

Financial support from the Academy of Finland and the Finnish Pharmaceutical Society are greatfully acknowledged. I also wish to thank Orion Pharma for giving me the opportunity to finalize my dissertation by working time arrangements.

During these years I've been lucky to work with great people both at the Division of Pharmaceutical Technology and at Orion Pharma. I would like to express warm thanks to all of you. I want to thank especially my first roommates in the legendary room of 'Johtajat'; Henna, Sanna, Kaisa and Anna for their warm welcome and for sharing the unforgettable atmosphere at the moments of joy and despair. I also wish to thank Anne for her friendship and Harri and Sanna for their patient guidance with the equipment in the lab. I would also like to take this opportunity to thank Johanna, Marja, Bert and many others from Orion for knocking on my door and picking me for lunch or coffee during my writing days. People at the LT 2nd floor coffee room deserve thanks for bringing something else into my mind during breaks and also for listening to my occasional bursts of whatever was going on at the moment.

Finally, I want to thank my family in Finnish. Kiitos, äiti Maija ja isä Jorma, että uskoitte minuun ja kannustitte eteenpäin kaikki nämä vuodet. Kiitos myös Tarulle ja Teijolle perheineen tuesta ja kaikesta iloisesta, mitä teidän kauttanne olen saanut kokea. Mummulle ja pappalle kiitos siitä, että olette odottaneet minua koulusta pienestä pitäen ja kiinnostuneina seuranneet taivaltani. Lopuksi haluan kiittää Jania – "ei mittä, ja kaik mitä ossan sanno".

Kirkkonummi, September 2011

Tarja Limnell

Contents

List of original publications

This thesis is based on the following publications, which are referred to in the text by their roman numerals **I-IV**:

I Limnell, T., Riikonen, J., Salonen, J., Kaukonen, A.M., Laitinen, L., Hirvonen, J., Lehto, V.-P., 2007. Surface chemistry and pore size affect carrier properties of mesoporous silicon microparticles. *International Journal of Pharmaceutics* 343: 141-147.

II Limnell, T., Heikkilä, T., Santos, H. A., Sistonen, S., Hellstén, S., Laaksonen, T., Peltonen, L., Kumar, N., Murzin, D. Y., Louhi-Kultanen, M., Salonen, J., Hirvonen, J., Lehto V.-P., 2011. Physicochemical stability of high indomethacin payload ordered mesoporous silica MCM-41 and SBA-15 microparticles. *International Journal of Pharmaceutics* 416: 242-251.

III Limnell, T., Santos, H. A., Mäkilä, E., Heikkilä, T., Salonen, J., Murzin, D. Y., Kumar, N., Laaksonen, T., Peltonen, L., Hirvonen, J., 2011. Drug delivery formulations of ordered and non-ordered mesoporous silica: Comparison of three drug loading methods. *Journal of Pharmaceutical Sciences* 100: 3294–3306.

IV Kaukonen, A. M., Laitinen, L., Salonen, J., Tuura, J., Heikkilä, T., Limnell, T., Hirvonen, J., Lehto, V.-P., 2007. Enhanced *in vitro* permeation of furosemide loaded into thermally carbonized mesoporous silicon (TCPSi) microparticles. *European Journal of Pharmaceutics and Biopharmaceutics* 66: 348-356.

The original publications were reprinted with permissions from the publishers. In publication **II** the first two authors contributed equally into the work.

Abbreviations and symbols

α_{OH}	silanol number
λ	wavelength
annTCPSi	annealed thermally carbonized porous silicon
annTOPSi	annealed thermally oxidized porous silicon
AP	apical
API	active pharmaceutical ingredient
BCS	Biopharmaceutics Classification System
BET	Brunauer-Emmett-Teller
BJH	Barrett-Joyner-Halenda
BL	basolateral
CD	cyclodextrin
CDER	Center for Drug Evaluation and Research
CTAB	cetyltrimethylammonium bromide
DSC	differential scanning calorimetry
DMSO	dimethylsulfoxide
e.g.	exempli gratia (for example)
EMEA	European Medicines Agency
EPAS	evaporative precipitation into aqueous solution
et al.	et alia (and others)
EtOH	ethanol
FDA	U.S. Food and Drug Administration
FHMG	fluidized hot-melt granulation
FTIR	Fourier transform infrared spectroscopy
GI	gastrointestinal
HBSS	Hank's balanced salt solution
HEPES	4-(2-Hydroxyethyl)piperazine-1-ethanesulfonic acid
HF	hydrofluoric acid
HIV	Human immunodeficiency virus
HPLC	High Performance Liquid Chromatography
HPMC	hydroxypropylmethylcellulose
IARC	International Agency for Research of Cancer
IMC	indomethacin
IUPAC	International Union of Pure and Applied Chemistry
logD	distribution coefficient
logP	partition coefficient
M41S	the family of mesoporous materials introduced by Mobil Oil company, USA
MCM	Mobil Composition of Matter
MCM-41	2-dimensional hexagonally ordered (*p*6*m*) mesoporous silica material synthesized with cationic surfactants as structure-directing agents, first reported by a research group at the Mobil Oil company, USA
MES	2-(N-Morpholino)ethanesulfonic acid
P_{app}	apparent permeability coefficient

PAMPA	parallel artificial membrane permeation assay
PEG	polyethylene glycol
pK_a	ionization constant
PSi	porous silicon
$PSiO_2$	porous silica
PVP	polyvinylpyrrolidone
RH	relative humidity
RRT	relative retention time
SBA-15	2-dimensional hexagonally ordered (*p*6*m*) mesoporous silica material synthesized with non-ionic triblock copolymers as structure-directing agents, first reported by a research group at the University of Santa Barbara, USA
SD	standard deviation
SEM	scanning electron microscopy
siRNA	small interfering ribonucleic acid
TCPSi	thermally carbonized porous silicon
TEER	transepithelial electrical resistance
TEOS	tetraethyl orthosilicate
THCPSi	thermally hydrocarbonized porous silicon
TOPSi	thermally oxidized porous silicon
w-%	per cent of weight
XRPD	X-ray powder diffraction

1 Introduction

The oral bioavailability of a drug is mainly determined by its solubility and permeability. In order to achieve effective oral medical treatment in patients, the drug molecule needs both to dissolve in the gastrointestinal (GI) tract and to permeate across the intestinal wall (Figure 1). These two phenomena (solubility and permeability) received well-deserved attention when the Biopharmaceutics Classification System (BCS) was introduced in 1995 to classify drugs according to their water solubility and membrane permeability (Amidon et al., 1995). Drug categorization according to the BCS has been widely employed as a tool to evaluate the developability and study requirements of drugs in both pharmaceutical industry and medicines regulatory agencies (CDER/FDA, 2000; Lennernäs and Abrahamsson, 2005; Dahan et al., 2009; EMEA, 2010). In addition to the molecular properties of a drug, the physicochemical and physiological conditions inside the GI-tract affect the drug bioavailability (Hörter and Dressman, 1997; DeSesso and Jacobson, 2001). There are inter- and intraspecies differences in those properties, which sometimes brings additional challenges to drug development.

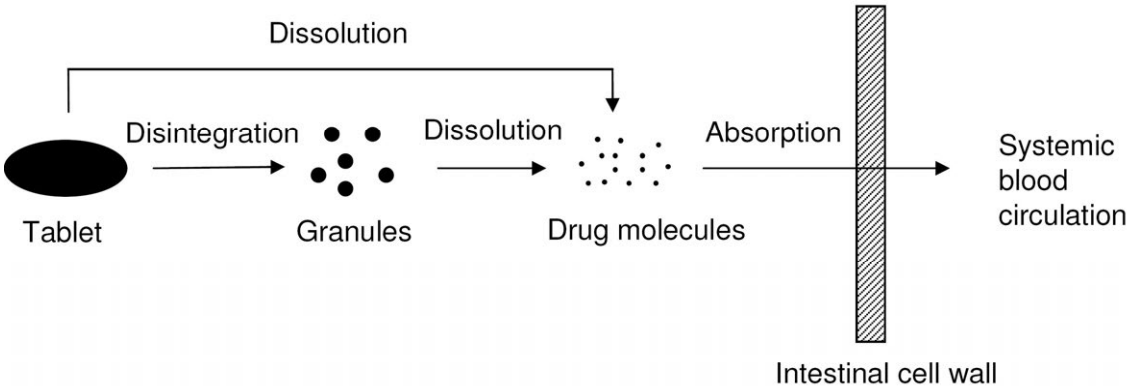

Figure 1. *Schematic diagram of the phases required for a drug in an oral dosage form to pass across the GI-tract in order to reach the systemic circulation. Adapted from (Aulton, 2002).*

Passive permeation of drugs can occur either through (transcellular route) or between (paracellular route) the cells (Hämäläinen and Frostell-Karlsson, 2004). The transcellular permeability is mostly a lipophilicity-related property of a molecule and it should be considered already during lead optimization phase of drug development (Kerns and Di, 2003). In order to improve the paracellular permeability of drugs some permeability enhancers (*e.g.*, chitosan and sodium caprate) for drug formulations have been studied, but their mechanisms of action often modify the cell membrane, which has raised concerns for their utilization in improved drug permeation (Artursson et al., 1994; Tomita et al., 1996; Gomez-Orellana, 2005).

The pharmaceutical means to improve oral drug bioavailability focus mainly on improving the drug solubility and dissolution rate (Fahr and Liu, 2007). This can be achieved by various methods, for example cyclodextrins (CD) are used as carriers for

lipophilic drugs. The drug molecule or, more frequently, its lipophilic moiety fits into the hydrophobic cavity of the CDs and the formed complex possesses improved solubility properties (Laza-Knoerr et al., 2010). The parameters that affect diffusion-controlled dissolution rate of solids can be described by the Noyes-Whitney equation [Eq. (1)], which can also be used to describe the dissolution of drugs (Aulton, 2002):

$$\frac{dC}{dt} = \frac{DA(C_s - C)}{h} \quad (1)$$

where *dC/dt* is the rate of dissolution of the drug particles, *D* is the diffusion coefficient of the drug in solution, *A* is the effective surface area of the solid, C_s is the saturation solubility of the drug in solution in the diffusion layer, *C* is the concentration of the drug in the solution and *h* is the thickness of the diffusion layer. A common technique to improve drug dissolution is to decrease the particle size of a drug by producing nanocrystals of the drug molecules (Shegokar and Müller, 2010). This increases the surface area of the drug, which in turn improves the drug dissolution rate as shown in Eq. (1). Lipid formulations have also been developed in order to improve the bioavailability of lipophilic active pharmaceutical ingredients (APIs) (Pouton, 2000; Porter et al., 2008). In these formulations the drug is often dissolved in the excipients. Thus, the dissolution phase is at least partly avoided and the drug is readily available for absorption via the intestinal/lymphatic route.

In addition, the solid state properties of a drug, which include different crystalline forms and amorphous disordered structures of the molecules, also strongly affect the dissolution rate (Hancock and Parks, 2000; Huang and Tong, 2004; Blagden et al., 2007). Crystal engineering includes, *e.g.*, crystal habit modifications (Adhiyaman and Basu, 2006), polymorph screening (Pudipeddi and Serajuddin, 2005) and co-crystal development (Vishweshwar et al., 2006). The dissolution of the amorphous form of a drug can be markedly better than that of its crystalline counterparts (Hancock and Parks, 2000). Although it has been under extensive studies for the last decades, the poor physical stability still remains the major drawback in the development of medicinal products containing amorphous APIs (Serajuddin, 1999; Yu, 2001). The amorphous state of a compound is thermodynamically less stable and has a tendency to convert into the more stable, crystalline form – thus affecting the drug dissolution rate. Different methods to produce stabilized amorphous formulations will be discussed in more detail later in this thesis.

One of the methods to improve the dissolution rate and permeability of drugs is to load the APIs into silicon/silica-based mesoporous materials, in which the crystallization of the loaded material is avoided by the restricted pore size of the materials and the interactions between the drug and the pore surfaces. According to the IUPAC (International Union of Pure and Applied Chemistry) definition, mesoporous materials have pore sizes between 2 and 50 nm (Rouquerol et al., 1994). The mesoporous particle sizes and shapes can vary. Porous silicon (PSi) materials were initially studied in non-pharmaceutical applications taking advantage of their light emitting properties towards applications as sensors (Canham, 1990; Lin et al., 1997; Stewart and Buriak, 2000). Applications of PSi as a

carrier of drugs have emerged later (Foraker et al., 2003; Salonen et al., 2005; Vaccari et al., 2006). Ordered mesoporous silicas, such as MCM-41 and SBA-15 (2-dimensional hexagonally ordered, *p*6*m*, mesoporous silica materials), were originally introduced as catalysts and adsorbents (Beck et al., 1992; Kresge et al., 1992; Zhao et al., 1998a). During the past decade, they have been widely studied in pharmaceutical and medical applications, including for example, delivery of drugs and proteins and bone tissue engineering (Han et al., 1999; Vallet-Regí et al., 2001; Vallet-Regí, 2006; Wang, 2009).

In vitro permeability experiments provide estimations on the *in vivo* absorption of drugs with less complex experimental settings and alleviated ethical issues when avoiding animal studies. The Caco-2 cell line derives from human colon adenocarcinoma and can be grown *in vitro* to resemble the small intestinal epithelium both structurally and functionally, including active transporters (Hilgers et al., 1990). It is a widely studied and utilized cell line for predicting intestinal absorption both in academia and in the industry (Hubatsch et al., 2007). Merely passive permeation of drugs can be also studied by PAMPA (Parallel Artificial Membrane Permeation Assay), a method designed for high throughput screening of new chemical entities (Kansy et al., 1998). Several other methods are also available for predicting *in vivo* permeability, such as surface plasmon resonance biosensor analysis and computer-aided *in silico* techniques (Hämäläinen and Frostell-Karlsson, 2004).

The objective of this dissertation was to study mesoporous silicon/silica-based materials as drug delivery vehicles for poorly water soluble drugs. This topic was accessed from different perspectives including: (i) the evaluation of different pharmaceutical drug loading methods for the particles; (ii) the ability of the materials to stabilize the drugs in a disordered form; (iii) improved drug dissolution; and (iv) enhanced drug permeability across the Caco-2 cell model. Finally, the mesoporous silica materials containing a model drug were formulated as pharmaceutical tablets in order to perform proof-of-concept evaluations of final dosage forms of these systems.

2 Review of the literature

2.1 Processing amorphous drug formulations

Drugs can exist in different polymorphic forms (Aulton, 2002; Huang and Tong, 2004). In crystalline forms the drug molecules are packed in a repeating long-range order and form a three-dimensional crystal lattice. Amorphous materials have no long-range order between the molecules and usually dissolve more rapidly than their crystalline forms. The stabilization of amorphous form is thus an interesting method to increase the drug dissolution rate.

Table 1. *Different methods for the preparation of stabilized amorphous formulations. Adapted e.g. from (Leuner and Dressman, 2000; Vasconcelos et al., 2007).*

Melt methods	**Solvent methods**	**Other methods**
• Melt quenching	• Spray drying	• Co-grinding
• Hot melt extrusion	• Freeze drying	• Adsorption on solid carrier
• Hot melt granulation	• Supercritical fluid method	• Evaporative precipitation into aqueous solutions
• Other melt methods	• Other melt methods	
• Spray congealing / cooling	• Spray freeze drying	
• Dropping method	• Spray coating in fluid bed	
• Direct capsule filling	• Electrostatic spinning method	

Despite decades of active research in the field, the physical stability of amorphous drugs still remains a challenge for pharmaceutical industry. Solid dispersions have been recognized as a potential method to stabilize the amorphous form of a drug, and several reviews have addressed this topic elsewhere (Chiou and Riegelman, 1971; Serajuddin, 1999; Leuner and Dressman, 2000; Vasconcelos et al., 2007; Kawakami, 2009). Solid dispersion was first introduced as a method to decrease crystalline particle size of sulfathiazole in a form of eutectic mixture with urea (Sekiguchi and Obi, 1961). Later, the term solid dispersion was defined as “the dispersion of one or more active ingredients in an inert carrier or matrix at solid state prepared by the melting (fusion), solvent, or melting-solvent method” (Chiou and Riegelman, 1971). In the same publication, the variations of the solid dispersions were classified according to the physical states of the mixture components. The work in this area has been rather active and some formulations have successfully reached the market (Janssens and Van den Mooter, 2009). The common feature in many of these products is an amorphous hydrophilic polymer carrier based on polyethylene glycol (PEG), polyvinylpyrrolidone (PVP) or cellulose derivatives. The miscibility of a drug into the selected polymer is an important factor affecting the success of the formulation (Qian et al., 2010). Failed combinations of polymers and drugs often

result in non-intentional crystallization of the drug during storage, which in turn leads to dissolution problems. Different approaches to process drugs into their stabilized amorphous forms will be discussed in the next chapters. Various methods to prepare stabilized amorphous formulations are summarised in Table 1.

2.1.1 Melt methods

Typically, in order to convert a crystalline API into its amorphous form by melt methods the material has to be heated above the melting point of the drug (Chiou and Riegelman, 1971). This makes most of the melt methods inappropriate for thermolabile APIs. At simplest, a melt method for preparing solid dispersions occurs by fusion. The carrier is melted and the drug incorporated into it followed by cooling either slowly or rapidly. The solid materials can also be mixed and melted together at the same time (Sekiguchi and Obi, 1961). Unless processed further, the melt hardens into the vessel and presents an additional challenge for formulation scientists. More convenient methods for preparing solid dispersions by melt method have also been developed as presented below.

Melt quenching

Melt quenching, also known as quench cooling, is a common way of producing amorphous APIs and solid dispersions, especially in laboratory scale (Andronis et al., 1997; Watanabe et al., 2001; Bahl and Bogner, 2006). In this method the amorphisation is achieved through melting the material and cooling it rapidly. Liquid nitrogen is usually utilized as the cooling aid to ensure fast enough solidification of the melt, which supports the formation of a glassy dispersion. In order to acquire processable mass for further studies, the cold hard solid dispersion needs to be gently ground. Melt quenching can also be combined with other processing methods, such as cryogrinding (Greco and Bogner, 2010).

Hot melt extrusion

In the hot melt extrusion process the solid dispersion components, possibly containing also additional excipients like plasticizers, are fed into a thermo-controlled screw system (Crowley et al., 2007). The materials are then melted to produce a homogenous dispersion as a result of the energy provided by heating and the pressure produced by the shear forces of the rotating screws (Breitenbach, 2002; Crowley et al., 2007). There are two main types of melt extruders: the single screw equipment, which is often favored for its simplicity, and the twin-screw extruders that possess more versatile possibilities to modify process parameters and the equipment composition. The extrusion process includes three principal functions: (1) feeding of the mass; (2) mixing and plasticizing the mass in the screw barrel; and (3) the flow of the processed mass through the final die to achieve the end product. Additional devices, such as process analytical equipment or mass flow feeders, can be included to further improve the control over the process. Hot melt extrusion can be utilized as a continuous process, which is a substantial benefit as compared to other methods of processing the amorphous materials (Repka et al., 2007). In order to convert

the crystalline API into amorphous form by hot melt extrusion, the material has to be heated above the melting point of the drug. However, plain amorphous API can also be used as a starting material in the hot melt extrusion process and, consequently, stabilized with appropriate polymer(s) at lower temperatures (Lakshman et al., 2008). This option makes the hot melt extrusion an important method for preparing solid dispersions also from thermolabile APIs. By adding supercritical carbon dioxide into the extruder, the macroscopic morphology of the formulation can be changed towards a foam-like structure, which has beneficial effects on the processability of the material (Verreck et al., 2005). Melt extrusion has been successfully implemented in some commercial pharmaceutical products such as Kaletra®, a protease inhibitor for the treatment of Human immunodeficiency virus (HIV) (Breitenbach, 2006).

Hot melt granulation

In early years, hot melt granulation has mainly been considered as an option for liquid-free processing (Thies and Kleinebudde, 1999; Vervaet and Remon, 2010). With the emerging challenges in the solubilities of the APIs, hot melt granulation has raised attention due to its utilizability in solid dispersion processing and its potential as a drug bioavailability enhancing technique (Seo et al., 2003; Walker et al., 2007; Passerini et al., 2010). Common pharmaceutical techniques, such as fluidized bed and high or low shear mixers, have been used in hot melt granulation in order to produce granules or agglomerates of API-carrier dispersions (Gupta et al., 2001; Passerini et al., 2002, 2010; Yang et al., 2007; Andrews, 2007). Early studies were mostly performed with high or low shear equipment, but studies with API-containing formulations using the fluidized hot-melt granulation (FHMG) are also starting to emerge (Walker et al., 2007; Patel and Suthar, 2009; Passerini et al., 2010). The FHMG has been successfully utilized in producing fast-release granules from cinnarizine, ibuprofen, and ketoprofen, which are poorly soluble BCS class II drugs. In order to solidify a solid dispersion in a manner that produces easily processable granules, the carrier and API are melted together, followed by spraying the melt onto a solid carrier in the high shear or fluid bed vessel (Seo et al., 2003; Holm et al., 2007). This technique is referred to as “pump-on” method. Another approach to melt granulation, so called “melt-in” method, includes the addition of the formulation components to the processing vessel and mixing those as solid dry powders, followed by heating and subsequent cooling. Depending on the process temperature, either the polymer alone or together with the API is melted in order to produce a dispersion (Perissutti et al., 2003; Walker et al., 2007). The crystallinity of the API in the produced granules varies according to the process parameters, *e.g.* temperature and shear forces, and the polymer/API ratios (Yang et al., 2007; Passerini et al., 2010).

Other melt methods

In spray congealing or cooling, the melted API-carrier dispersion is sprayed into a receiving vessel, where it solidifies into small particles (Rodriguez et al., 1999; Passerini et al., 2006; Jannin et al., 2008). The receiving vessel can be either cooled or at room temperature depending on the equipment and the used carrier. The melted solid dispersion can also be manually pipetted onto a plate as droplets which then solidify into particles

(Bülau and Ulrich, 1997; Bashiri-Shahroodi et al., 2008). When the melt is pipetted directly into a gelatine capsule, the process is called “direct capsule filling” (Francois and Jones, 1978).

2.1.2 Solvent methods

Solvent methods for the manufacturing of solid dispersions require that both the drug and the carrier dissolve into the same solvent system, which may contain one or more solvents. The solvent can then be evaporated by various means; the simplest is by leaving the vessel open or by using, for example, rotary evaporator (Betageri and Makarla, 1995). More sophisticated methods are presented in the next paragraphs.

Spray-drying
Evaporation of the solvents in the spray dryer occurs as atomized droplets of the solution are fed into a heated gas flow (Cal and Sollohub, 2010). The process can be optimized by adjusting the temperature and flow of the solution and the gas. In spray-drying the material dries fast, which supports the formation of the amorphous product. Spray-drying has been successfully utilized in the production of various solid dispersions (Yonemochi et al., 1999; Takeuchi et al., 2005; Shen et al., 2009; Sollohub and Cal, 2010).

Freeze-drying
Freeze-drying, also known as lyophilization, is a method where the solution is first freezed, *e.g.* in liquid nitrogen, and the frozen solvents are then removed via sublimation in a reduced pressure (Rowe, 1960; Tang and Pikal, 2004). As the process includes many stages, it is usually slower than spray-drying. The lyophilized material had the most advantageous dissolution properties when compared to solid dispersions produced by melt method and solvent method utilizing rotavapor (Betageri and Makarla, 1995).

Supercritical fluid method
One option for producing solid dispersions without organic solvents or extreme temperatures is supercritical fluid processing. The supercritical fluid can be used as a solvent or as an antisolvent in order to produce solid dispersions; the processes slightly vary depending on the approach taken. They may include also melting or dissolving the drug in an organic solvent (Karanth et al., 2006). Carbon dioxide has many beneficial properties, such as being nontoxic, non-flammable, and inexpensive. All these combined with reasonable critical temperature and pressure makes carbon dioxide the most commonly used supercritical fluid in the pharmaceutical field (Sethia and Squillante, 2002; Karanth et al., 2006). Various solid dispersion formulations have been prepared via supercritical fluid processing (Sethia and Squillante, 2002; Gong et al., 2005; Miura et al., 2010). As an example, *in vivo* evaluation of the supercritical fluid formulation surpassed the solid dispersion prepared by the traditional solvent evaporation method (Miura et al., 2010).

Other solvent methods

Spray-freeze-drying method combines processing steps common to the freeze-drying and spray-drying methods. In spray-freeze-drying a solution of API and the carrier is first sprayed onto liquid nitrogen. The frozen droplets are then dried in a freeze dryer (van Drooge et al., 2005). By this method, round solid dispersion particles can be produced without heating, which favors this process especially when using thermolabile APIs. Due to the round shape of the end products, the spray-freeze-drying is often used to produce inhalable solid dispersions (van Drooge et al., 2005; Zijlstra et al., 2007). In oral dosing the great advantage of this method has been proven *in vivo* against solid dispersions produced by rotavapor and commercially available tablets (He et al., 2011; Tong et al., 2011).

The API-carrier solution can also be sprayed on the surface of sugar beads or other excipients in fluidized bed. This method is called spray-coating in fluid bed. The release profile of the acquired pellets or granules can be modified by selecting the carrier type and API/carrier ratio (Beten et al., 1995; Ho et al., 1996). Spray-coating in fluid bed has been proven effective in the production of commercial antifungal itraconazole formulation Sporanox® (Gilis et al., 1997).

Another solvent method is the electrostatic spinning method, where a solution of API and polymer is exposed to high voltages (Doshi and Reneker, 1995; Kenawy et al., 2002; Yu et al., 2009b). The solvent evaporates during the process and the fiber-like solid end-product can be further processed. Some promising results have been achieved for improving the solubility of poorly soluble drugs by using solid dispersions prepared by the electrostatic spinning (Verreck et al., 2003; Yu et al., 2009a, 2010).

2.1.3 Other methods

Co-grinding an API with a solid dispersion carrier has also been used to produce amorphous formulations (Watanabe et al., 2003; Bahl and Bogner, 2006). The carrier material can be porous when the API adsorbs to the large surface of the material, for example, onto porous silica ($PSiO_2$) or silicon (PSi) materials. In this dissertation, the adsorption on solid carriers has also been used as a method to improve the solubility of APIs. In addition to co-grinding, the adsorption of APIs onto porous materials can also be performed with some of the techniques described above as such, or with slight modifications (Li et al., 2002; Smirnova et al., 2003; Heikkilä et al., 2007b; Mellaerts et al., 2008a; Shen et al., 2009).

Evaporative precipitation into aqueous solutions (EPAS) is a method where a heated organic solution of a drug is sprayed into heated aqueous solution (Sarkari et al., 2002). The organic solvent evaporates rapidly leading to the supersaturation and precipitation of the drug. Stabilizing excipients are present in either of the solutions. The aqueous phase is subsequently removed, *e.g.* by spray-drying. Rapid dissolution of the particles has been commonly observed, despite the variation in the crystallinity of the APIs (Sarkari et al., 2002; Chen et al., 2004; Sinswat et al., 2005). The small size of the particles prepared via EPAS has also a beneficial effect on the drug dissolution rate.

2.2 Properties of mesoporous silicon and silica materials

2.2.1 Methods of fabrication

Mesoporous materials have pore sizes between 2 and 50 nm but their particle sizes and shapes can vary (Rouquerol et al., 1994). In general, nanomaterials can be fabricated according to two different principles (Euliss et al., 2006; Shegokar and Müller, 2010): the first one is a top-down approach, where the larger starting material is processed into smaller fractions by various mechanisms such as milling; and the second one is a bottom-up approach involving sophisticated build-up of complex structures starting from a molecular level. Similar principles are utilized in the fabrication of PSi and $PSiO_2$.

Porous silicon (PSi) materials are produced by a top-down approach (Canham, 1990; Salonen et al., 2008; Salonen and Lehto, 2008; Anglin et al., 2008). The most common way to produce PSi is by electrochemical anodization. In this method the Si plate functions as an anode in the system and is immersed in a hydrofluoric acid (HF) solution together with a platinum plate, which serves as cathode. The pore formation on the surfaces of the silicon is enforced via etching current. The outcome of the process is strongly dependent on the fabrication conditions, which can then be utilized in tuning the pore properties of the porous materials. For example, the achieved pore size and surface area are affected by the electrolyte composition and the applied current density during the electrochemical etching (Salonen et al., 2000a). Another means to fabricate PSi is stain-etching, a process that resembles the electrochemical etching with the exception that it utilizes chemicals instead of electrical bias (Shih et al., 1992; Fathauer et al., 1992) and photosynthesis, where visible light together with HF is used to produce PSi (Noguchi and Suemune, 1993). One of the most recent published methods to produce PSi is by the solid flame technique (Won et al., 2009). In this method the PSi is formed as SiO_2 reacts with Mg in a combustion chamber followed by an acid treatment. PSi has also been fabricated by using the ball-milling technique combined with pressing and sintering procedures (Jakubowicz et al., 2007).

Various $PSiO_2$ materials are produced by bottom-up methods. Depending on the selected manufacturing components and conditions, the resulting material is either silica gel with non-ordered pore structure or a more structured, ordered silica material. Sol-gel processing is utilized in the syntheses of both $PSiO_2$ materials discussed here. The “sol” is described as a colloidal suspension of the silica, while the “gel” forms as the silica concentration of the suspension raises above a limit where an interconnected network is formed (Iler, 1979; Hench and West, 1990).

Silica gel is often formed from alkoxide precursors $Si(OR)_4$, such as tetraethoxysilane (TEOS) in aqueous environment. The alkoxysilanes undergo hydrolysis followed by condensation forming reactive ≡Si-O-Si≡ molecular bonds. When these molecular bonds react with additional silanol groups, a silica network begins to grow. The polymerization process starts with the polymerization of monomers which grow into primary particles. According to the Ostwald ripening mechanism, the smaller particles dissolve and the dissolved molecules attach to the surfaces of the larger particles. Subsequently, these

particles grow and finally start to interconnect forming chains and a three-dimensional network. The growth of single particles and the amount of cross-linking between the particles depends on the pH and the molar ratio of water and alkoxides in the “sol”. The prepared gel is then dried and the final xerogel, silica gel, is formed. (Iler, 1979; Brinker and Scherer, 1990; Hench and West, 1990)

Ordered mesoporous silica synthesis processes utilize different template systems to direct the silica molecules into a mesoscopically ordered yet amorphous structure (Rigby et al., 2008). The dawn of the ordered mesoporous silica research is considered to have begun from the studies of Mobil Corporation scientists in 1992 (Beck et al., 1992; Kresge et al., 1992). They used alkyltrimethylammonium ion surfactants to form the templates for unidirectional hexagonal silica networks, named MCM-41, of the family of M41S materials. The pore size of these materials can be modified by selecting the alkyl chain length or by adding some auxiliary hydrocarbons to the synthesis. In addition to the ammonium-based surfactants, amphiphilic block copolymers can also function as structure-directing agents. The first polymer-templated ordered hexagonal material was named as SBA-15 (Zhao et al., 1998a, 1998b). The pore size can also be fine-tuned with polymer templates. This occurs by varying the heating temperature, the cosolvent amount or the time of the synthesis. The achievable maximum pore size is larger when polymers are used as templates than with smaller surfactant systems. After the synthesis, the templating material needs to be removed. This can be achieved by calcination under nitrogen flow or by solvent extraction (Kresge et al., 1992; Slowing et al., 2008). The two main proposed pathways for the mechanisms of the ordered mesoporous silica synthesis included, (1) a self arrangement of the templating structure, followed by incorporation of silica to form a porous network, and (2) a combined involvement of the template and silica in the formation of the surfactant micelle structures covered by silica.

The morphology of the materials can be modified by changing the synthesis conditions; for example, stirring of the synthesis solution produced fiber-like SBA-15, whereas rod-like material was the product of the still synthesis solution (Kosuge et al., 2004). The templating system has also been adapted to produce the Hiroshima Mesoporous Material, which is spherical mesoporous silica synthesized inside micelles containing *in situ* forming polystyrene as a template for the mesoporous structure (Nandiyanto et al., 2009).

2.2.2 Structural differences

Mesoporous silicon/silica-based materials provide a possibility to tailor the carrier structure and the surface composition according to the different needs. The pore size can be modified to fit the size of the drug molecule that will be loaded into the porous material, as well as to achieve the aimed release profile. The release profile can be controlled also via different surface treatments of the materials, leading to desired interactions between the porous carrier and the loaded substance. The surface treatment can also affect the loading of the molecules into the pores via hydrophobic-hydrophilic interactions. The next paragraphs will discuss the characteristic pore morphology and

surface chemistry of mesoporous silicon and silica materials. The effects of these properties and their modifications on drug delivery are discussed later on in this thesis.

2.2.2.1 Pore morphology

The fabrication method used affects the structural order of the pores in each material. Silica gel is formed via condensation polymerization and the material is composed of non-ordered silica network resembling a sponge-like structure (Iler, 1979). The porosity can be slightly modified by adapting the synthesis conditions; however the outcome is amorphous, irregular $PSiO_2$ with variable pore size and shape. The pore structure of PSi depends on the fabrication conditions including, for example, the type of the silicon source, current density and HF concentration used (Lehmann et al., 2000; Salonen et al., 2008). Generally, one can conclude that with lower current densities the pores are more tortuous, fir tree or sponge-like, and with increasing current densities the pores become wider and more linear. A schematic example of one possible mesopore structure of PSi is shown in Figure 2A. The pore diameters of PSi can vary from few nanometers to micrometers, however in drug delivery the mesoporous silicon is the most studied (Lehmann and Grüning, 1997; Salonen et al., 2005, 2008). In addition, many parameters affect the pore diameter, which in turn can be adjusted to optimize the pore properties. The pore size distribution of PSi is usually wider than that of mesoporous silicas, whose pore sizes mainly depend on the utilized template materials (Kresge et al., 1992; Salonen et al., 2008). The definite advantage of mesoporous silicas is their uniform pore sizes which can be tailored by selecting an appropriate template system (Beck et al., 1992; Zhao et al., 1998b). The most studied mesoporous silicas in drug delivery applications are MCM-41 and SBA-15 materials. They exhibit highly ordered two-dimensional tube-like pore structures (Figure 2B). MCM-41 pore diameter lies typically between 1.5 and 10 nm, whereas polymer-templated SBA-15 has wider pores of 4.6-30 nm. The initial publications of ordered mesoporous silica presented these two-dimensional hexagonal structures (Kresge et al., 1992; Zhao et al., 1998a). The versatile templating systems enable various silica network assemblies, such as cubic or three-dimensional hexagonal ordered $PSiO_2$ structures; also several variable ordered silica materials have been reported (Beck et al., 1992; Tanev and Pinnavaia, 1995; Zhao et al., 1998b; Boissière et al., 2000; Wang, 2009).

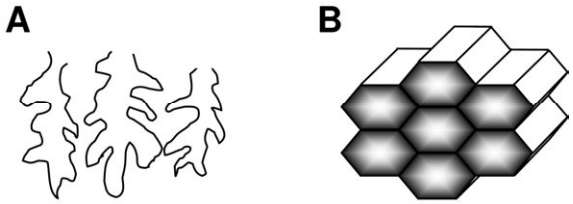

Figure 2. *Schematic representations of the mesopores of PSi (A) and ordered mesoporous SiO_2 (B). Adapted from (Kresge et al., 1992; Lehmann et al., 2000).*

2.2.2.2 Surface chemistry

Surface interactions between the porous particle and the loaded substance are critical in adjusting the pharmaceutical functions of the material. The surface areas of freshly-made mesoporous silicon, silica gel and ordered silica are about 300 m^2/g, 10-1000 m^2/g and >700 m^2/g, respectively (Beck et al., 1992; Zhao et al., 1998b; Zhuravlev, 2000; Salonen et al., 2005).

The as-anodized surface of PSi contains hydrides (Si-H, $Si-H_2$ and $Si-H_3$), which are prone to spontaneous oxidation in ambient air (Burrows et al., 1988; Canham et al., 1991; Salonen et al., 2008; Salonen and Lehto, 2008). The freshly made surface can be stabilized by converting the reactive groups into more stable oxidized, hydrosilylated or (hydro)carbonized forms (Figure 3).

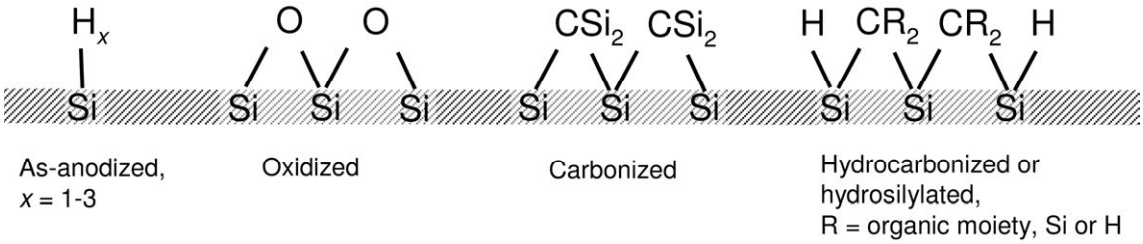

Figure 3. *Surface chemistry of mesoporous silicon after anodization and various surface treatments.*

Thermal oxidation is one of the simplest ways to oxidize silicon surfaces; the product is called thermally oxidized PSi (TOPSi) (Petrova-Koch et al., 1992; Salonen and Lehto, 1997). Other methods include, for example, chemical (Mattei et al., 2000) and anodic (Halimaoui et al., 1991) oxidation. The Si-C bond is kinetically more stable than the oxidized Si-O bond (Linford and Chidsey, 1993). The stabilization can be achieved by a catalyzed reaction of terminal alkenes or alkynes with the hydrides of silicon, called hydrosilylation. The hydrosilylation method can also be used to functionalize the surface of PSi for different purposes by using selected organic moieties in the other end of the alkene or alkyne (Buriak and Allen, 1998; Boukherroub et al., 2003). It is worth noting that the PSi surface is not entirely covered by hydrosilylation and some free hydrides usually remain. The same issue is encountered when Si-C bonds are formed via grafting reactions in solutions using organolithium or Grignard reagents (Bansal et al., 1996; Song and Sailor, 1998). A complete carbonization of the PSi surface can be achieved via thermal carbonization in the presence of gaseous hydrocarbon acetylene (thermally carbonized PSi, TCPSi) (Salonen et al., 2000b). At treatment temperatures below 700 °C, the hydrogen atoms remain on the PSi surface making it hydrophobic (Si-C-H bonds; thermally hydrocarbonized PSi, THCPSi). When the temperature is above 700 °C the formed surface is hydrogen free and more hydrophilic than the material produced at lower temperatures (Salonen et al., 2000b, 2004).

The surface of amorphous silica is covered with silanol (≡Si-OH) and siloxane (≡Si-O-Si≡) groups (Zhuravlev, 2000). In addition, there are structurally bound water molecules

inside the silica network, called internal silanol groups. The silanols can exist in three different forms: isolated, vicinal and geminal as shown in Figure 4. Isolated and geminal silanol groups can be used as grafting templates for, *e.g.* amino or dendrimer functionalized silica (Zhao and Lu, 1998; Muñoz et al., 2003; Reynhardt et al., 2005). The functionalization can also be performed during synthesis of the material as a co-condensation process (Huh et al., 2005; Radu et al., 2005). Silanol and siloxane groups can also interact as such with the loaded substances to form hydrogen bonds (Bahl and Bogner, 2006).

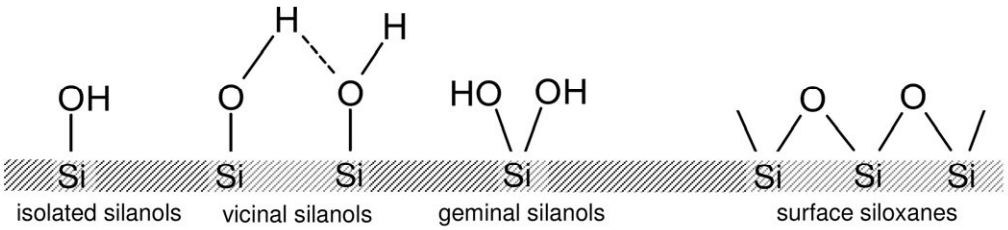

Figure 4. *Structures of the silanol and siloxane groups present on the amorphous silica surface. Adapted from (Zhuravlev, 2000).*

Silanol number, α_{OH}, is used to describe the number of OH groups per unit surface area of the silica materials. The value varies between different silica materials and is also affected by the post-synthetic treatments, such as the calcination time of the material (Zhao et al., 1997; Kozlova and Kirik, 2010). This makes the comparison of various results challenging, but generally, α_{OH} is the highest in amorphous silica gel (4.2-5.7), with decreasing values from SBA-15 (2.8-5.3) to MCM-41 (1.4-3) materials (Zhuravlev, 1987; Zhao et al., 1997; Shenderovich et al., 2003; Kozlova and Kirik, 2010).

2.2.3 Biological safety

Silicon is one of the most abundant chemical elements on the Earth's crust, usually present as silicon dioxide, silica (Yaroshevsky, 2006). The exact role of silicon in human biology is still under investigation. It is absorbed daily from food in the form of orthosilicic acid [$Si(OH)_4$], and its positive role in the health of connective tissues and bone has been recognized (Jugdaohsingh et al., 2002, 2003; Sripanyakorn et al., 2005). Silicon does not accumulate in the body; instead, it is readily excreted into urine as orthosilicic acid (Reffitt et al., 1999).

An unavoidable thought when it comes to dosing of silicon/silica-based materials to humans is silicosis – a respiratory disease derived from breathing of crystalline silica dust. Other diseases, such as lung cancer and rheumatoid arthritis, have also been connected to crystalline silica exposure (Calvert et al., 2003). It is important to recognize the difference between crystalline and amorphous silica. The International Agency for Research of

Cancer (IARC) has classified inhaled crystalline silica as carcinogenic to humans, but amorphous silica is not classifiable as to its carcinogenicity to humans (IARC 1997). Silicon dioxides are generally recognized as safe food substances and listed in the FDA (U.S. Food and Drug Administration) inactive ingredients database as used in, *e.g.*, oral and topical drug products (FDA, 1979, 2011). Probably due to the history of crystalline silica, human safety studies with amorphous silica have also mainly focused on pulmonary exposure (Merget et al., 2002). Some reversible lung symptoms have been reported, but no evidence of chronic diseases has been proven. On the other hand, chronic pulmonary effects have not been definitely excluded. The mechanism behind the better lung tolerability towards amorphous silica could be its higher surface area, which leads to faster dissolution and removal from the alveoli as compared to crystalline silica (Borm et al., 2004). However, the mechanism remains unclear and is not fully understood yet. The emergence of mesoporous silicon/silica-based materials as drug delivery systems has promoted the safety studies in the field.

2.2.3.1 In vitro studies

It has been noticed that highly porous silicon (porosity > 70%) dissolves in simulated body fluids excluding acidic simulated gastric fluid, whereas silicon with lower porosity is bioactive and allows the growing of hydroxyapatite on its surface (Canham and Reeves, 1995; Anderson et al., 2003; Salonen and Lehto, 2008). Anderson and co-workers studied the dissolution of PSi in order to develop it as a source of orthosilicic acid for absorption from the digestive tract (Anderson et al., 2003). The dissolution rate of PSi increased with the porosity of the material as well as with the pH and temperature of the dissolving medium.

The toxicity of the PSi materials with different surface treatments and morphologies has been studied with few cell lines (Figure 5 and Table 2). Interactions of the PSi-derived materials have been studied *in vitro* with intestinal Caco-2 cells, while inflammatory and immune responses and cellular uptake have been studied in human blood derived monocytes and RAW 264.7 murine macrophages (Ainslie et al., 2008; Bimbo et al., 2010; Santos et al., 2010). THCPSi particles were studied in several size fractions ranging from 97 nm to 25 µm and concentrations ranging from 15 to 250 µg/ml (Bimbo et al., 2010). The material was not considered to present significant toxicity, oxidative stress or inflammatory response in both Caco-2 and RAW 264.7 macrophage cells during 24 h. However, in some cases, decreased cell viabilities were observed. A similar study was also performed with TOPSi particles (Bimbo et al., 2011). Evidence of particle size and concentration dependent safety issues was observed, but the PSi particles of 164 nm appeared to be the safest particles in terms of toxicity. The particles did not pass through the Caco-2 cell membrane, but were phagocytised by RAW 264.7 macrophage cells, which could also be seen as slightly pronounced oxidative stress and inflammatory responses in the macrophages. An *in vitro* study comparing different properties of the PSi materials, such as different surface chemistries (Si-C, Si-O and Si-C-H), particle sizes (1.2-75 µm) and concentrations (0.2-4 mg/ml), and their influence in Caco-2 cell viability

after variable exposure times (3, 11 and 24 h) demonstrated the role of each of those properties in cell toxicity (Santos et al., 2010). All of the studied materials were considered acceptable for oral drug delivery development with certain limitations. The small particle sizes and the surface treatment were raised as the main contributors to the cytotoxicity, with the TOPSi surfaces appearing to be the safest materials in terms of toxicity regardless of the particles sizes. High particle concentrations caused more interference on the cell integrity and the effect was more pronounced with the THCPSi and TCPSi particles than with the TOPSi particles. The immune response of PSi materials has also been studied with human blood derived monocytes, where the biocompatibility of various PSi morphologies was observed to give similar responses as those of tissue culture polystyrene (Ainslie et al., 2008). In another study, the cytotoxicity of non-porous silicon nano- and microparticles (3 nm and 100-3,000 nm, respectively) was observed at concentrations above 20 and 200 µg/ml, respectively (Choi et al., 2009). So far, the *in vitro* safety of PSi materials has been shown satisfactory in the few studies performed. However, the particle size, dose and surface treatment of the PSi should be carefully considered for each potential *in vivo* application.

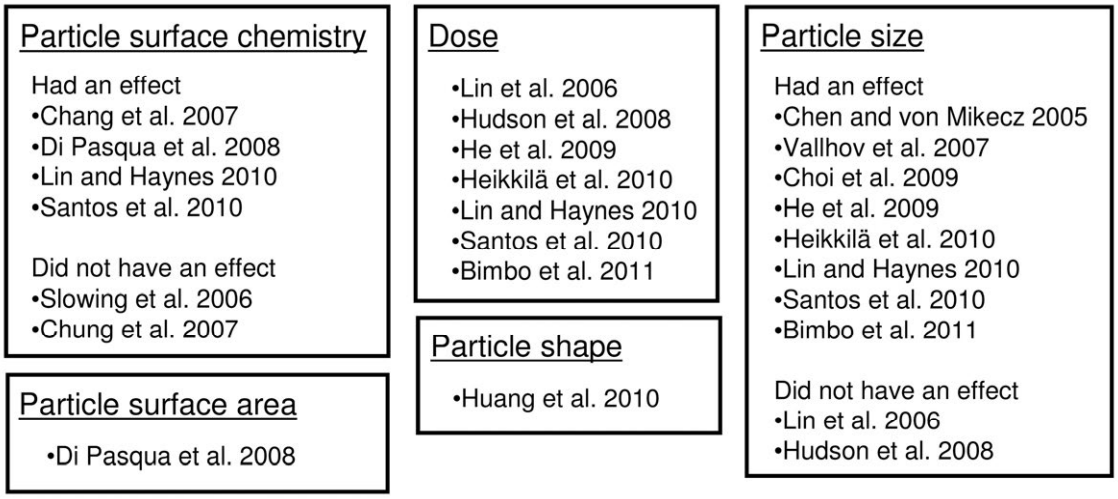

Figure 5. *Properties that are suggested to affect the in vitro $PSiO_2$ and PSi safety. References to the original studies are also provided.*

The safety of amorphous nano- and micronized, porous and nonporous silica, have been studied *in vitro* with variable results (Figure 5). In many studies, the size of the mesoporous silica has been shown to affect the cytotoxicity (Chen and von Mikecz, 2005; Vallhov et al., 2007; He et al., 2009; Choi et al., 2009; Heikkilä et al., 2010; Lin and Haynes, 2010; Santos et al., 2010; Bimbo et al., 2011). A toxic dose-dependent response has also been a common observation in many studies (Lin et al., 2006; Hudson et al., 2008; He et al., 2009; Heikkilä et al., 2010; Lin and Haynes, 2010; Santos et al., 2010; Bimbo et al., 2011). The toxicity studies of inhaled crystalline silica derived mainly from occupational basis and are focused on micron-sized particles (Fenoglio et al., 2000; Calvert et al., 2003). Recently, the nano-sized materials have also been under

investigation. The cytotoxicity of nano-sized, non-porous amorphous silica has been shown in human lung cancer cells (Lin et al., 2006). The observed effect was dose-dependent (10-100 µg/ml), but gave a similar response for the studied size-fractions (15 nm and 46 nm). When mesoporous and nonporous silica nanoparticles were compared, they both showed a dose- and size-dependent hemolytic activity on red blood cells, with the smaller size and higher concentrations inducing the stronger effects (Lin and Haynes, 2010). The studies were performed with 3.125–1600 µg/ml concentrations and particle sizes of ~25-260 nm. The hemolytic activity was lower with mesoporous silica than with the nonporous silica, and increased when the porosity of the material was destroyed. Grafting the silica surfaces with PEG reduced the observed effect. An increase in cytotoxicity with decreasing mesoporous particle size (190 nm – 1.22 µm) and increasing particle concentration has also been reported elsewhere (He et al., 2009). The study showed that calcinated materials are safer than the ones where the templating material has been removed by extraction. Partly opposite results were obtained with human monocyte-derived dendritic cells exposed to nano-sized (270 nm) and micron-sized (2.5 µm) mesoporous silica (Vallhov et al., 2007). In this case, the larger particles with high concentrations compromised the cell integrity more than the smaller particles, although the overall effect was considered minor with regard to further development of the materials as drug delivery systems. Micron scale (1-160 µm) MCM-41 and SBA-15 particles have been shown to cause cytotoxicity in Caco-2 cells at various doses (0.2-14 mg/ml) and after different exposure times (3 and 24 h) (Heikkilä et al., 2010). In that study, the smallest size fractions and the largest doses had the strongest effects on the studied parameters, including cell membrane integrity, metabolic activity, and apoptosis tendency of the cells. On the other hand, the influence of the larger size particle fractions was variable. In another study, no size dependence was seen comparing mesoporous silica between 150 nm and 4 µm in human mesothelial cells, mouse peritoneal macrophages, and mouse myoblasts differentiated into muscle cells (Hudson et al., 2008). The macrophages were least affected by the silica, whereas all the other cell lines showed decreased viability with increasing doses and duration of the exposure times of the cells to the particles. On average, silica nanoparticles of 12 nm have been shown to induce oxidative stress in RAW 264.7 macrophage cells at doses of 5-40 µg/ml (Park and Park, 2009), and the same observation has also been made for human umbilical vein endothelial cells exposed to silica particles of 20 nm and doses above 50 µg/ml (Liu and Sun, 2010). Negative impact on cellular respiration has been reported with both SBA-15 and MCM-41 (for particle sizes of hundreds of nanometers), with lesser extent to the latter particles due to the limited access to the mitochondria (Tao et al., 2008).

Table 2. *Summary of the in vitro safety studies performed with Si / SiO_2-based materials.*

Material	Cell line	Particle size	Dose	Reference
Si flat, nanoporous Si, nanochanneled Si and micropeaked Si	human blood-derived monocytes	n.a.	n.a.	(Ainslie et al. 2008)
THCPSi	human colon carcinoma (Caco-2) and murine macrophage (RAW 264.7)	97 nm - 25 µm	15 - 250 µg/ml	(Bimbo et al. 2010)
TOPSi	human colon carcinoma (Caco-2) and murine macrophage (RAW 264.7)	97 nm - 25 µm	15 - 250 µg/ml	(Bimbo et al. 2011)
TCPSi, TOPSi and THCPSi	human colon carcinoma (Caco-2)	1.2 – 75 µm	200 - 4000 µg/ml	(Santos et al. 2010)
non-porous silicon	murine macrophage (RAW 264.7)	3 nm and 100 - 3000 nm	1 - 200 µg/ml	(Choi et al. 2009)
mesoporous silica	mouse fibroblasts (3T3-L1)	110 nm	n.a.	(Lin et al. 2005)
mesoporous silica	human cervical cancer cell (HeLa)	~150 nm	100 µg/ml	(Slowing et al. 2006)
mesoporous silica	human mesenchymal stem cells (hMSCs) and mouse adipocytes (3T3-L1)	~100 nm	100 µg/ml	(Chung et al. 2007)
mesoporous silica	human monocyte-derived dendritic cells	270 nm and 2.5 µm	0.5 - 50 µg/ml	(Vallhov et al. 2007)
mesoporous silica	human neuroblastoma cells (SK–N–SH)	~250 nm	40 - 800 µg/ml	(Di Pasqua et al. 2008)
mesoporous silica	human mesothelial cells (ATCC, MeT-5a), mouse peritoneal macrophage cells (ATCC, PMJ2-PC) and mouse myoblast cells, differentiated into muscle cells (ATCC, C2C12)	~150 - ~4000 nm	100 - 500 µg/ml	(Hudson et al. 2008)
mesoporous silica	HL-60 (myeloid) cells and Jurkat (lymphoid) cells	hundreds of nanometers	50 - 200 µg/ml	(Tao et al. 2008)
mesoporous silica	human breast-cancer cells (MDA-MB-468) and African green monkey kidney cells (COS-7)	190 - 1220 nm	10 - 480 µg/ml	(He et al. 2009)
mesoporous silica	human colon carcinoma (Caco-2)	1 - 160 µm	200 - 14000 µg/ml	(Heikkilä et al. 2010)
mesoporous silica	human melanoma cells (A375)	100 - 450 nm	50 - 1000 µg/ml	(Huang et al. 2010)
mesoporous silica and non-porous amorphous silica	human red blood cells	~25 - ~260 nm	3.125 - 1600 µg/ml	(Lin and Haynes 2010)
non-porous silica	human epithelial cells (HEp-2), epithelial, human nasal septum cells (RPMI 2650), human lung epithelial cells (A549), rat lung epithelial cells (RLE-6TN) and mouse brain neuroblast cells (N2a)	0.05 - 5 µm	25 µg/ml	(Chen and von Mikecz 2005)
non-porous silica	human bronchoalveolar carcinoma-derived cells (A549)	15 ± 5 nm and 46 ± 12 nm	10 - 100 µg/ml	(Lin et al. 2006)
non-porous silica	human fibroblast (CCD-966sk, WS1, MRC-5) and human epithelial (A549, HT-29, MKN-28)	~22 - 80 nm (aggregates ~188 - 236 nm)	21 - 4000 µg/ml	(Chang et al. 2007)
non-porous silica	murine macrophage (RAW 264.7)	~12 nm	5 - 40 µg/ml	(Park and Park 2009)
non-porous silica	human umbilical vein endothelial cells	20 nm	25 - 200 µg/ml	(Liu and Sun 2010)

The shape and surface properties of the mesoporous silica materials also affect their internalization and cytotoxicity. The effects vary from toxic to non-toxic depending on the cell lines and surface treatments used. Recently, the uptake of silica nanoparticles into various human, rat and murine cells was reported with sizes ranging from 40 nm to 5 µm (Chen and von Mikecz, 2005). The studies were performed with particle suspensions of 25 µg/ml, and penetration of the particles into the nucleus was detected only for sizes of 40-70 nm, while all the particles were able to pass the cell membrane into the cytoplasm. The particles induced formation of protein aggregates in the nucleoplasm, which is harmful for normal cell functions. Another study showed internalization of mesoporous silica nanoparticles (~110 nm) containing attached fluorescein dye into 3T3-L1 fibroblast cells' cytoplasms after one hour of exposure with no evidence of cellular damage (Lin et al., 2005). The shape of the particles also affected the internalization extent and rate into A375 human melanoma cells (Huang et al., 2010). Mesoporous silica particles with higher aspect ratio (*i.e.* length/width) had a stronger effect on the cell functions than the rounder particles in terms of, *e.g.* cell proliferation and apoptosis. Toxicity studies of MCM-41 particles and surface treated counterparts with human neuroblastoma cells (SK–N–SH) suggested that decreasing the surface area of the material improves safety, as well as the surface functionalization of the material (Di Pasqua et al., 2008). Chang and co-workers showed that cancer epithelial cells that proliferate faster than normal fibroblasts are less sensitive to silica exposures (Chang et al., 2007). The same study also suggested that the silica nanoparticles exhibit toxicity at concentrations above 138 µg/ml, although the cytotoxicity of silica could be reduced by surface treatment with chitosan. The increasing surface charge of MCM-41 nanoparticles (~100 nm) improved to some extent their uptake into both human mesenchymal stem cells and 3T3-L1 fibroblast cells (Chung et al., 2007). The particles with various surface charges did not affect the cell functions. Similar results have also been obtained with surface-functionalized MCM-41 in human cervical cancer cells (Slowing et al., 2006).

The *in vitro* safety studies with mesoporous silicon/silica-based materials are variable with regard to the studied materials, cell lines and treatments, as summarized in Table 2. Few critical parameters related to the *in vitro* cytotoxicity of mesoporous silica and PSi have been identified (Figure 5). The *in vivo* response to the materials will be discussed in the following chapter.

2.2.3.2 In vivo studies

Mesoporous silicon has been recognized as a non-toxic and feasible material for drug delivery in several *in vivo* studies. Since the early investigations using implants of large PSi disks (Bowditch et al., 1999; Rosengren et al., 2000), materials ranging from nano- to micron-sizes have been administered orally, subcutaneously and intravenously to rodents in order to access the safety information of plain or surface modified PSi (Park et al., 2009; Tanaka et al., 2010a, 2010b; Bimbo et al., 2010; Chiappini et al., 2011).

THCPSi (average particle size of 142 nm) did not cross the intestinal cell wall after oral administration in rats (Bimbo et al., 2010). This makes the material a promising

vehicle for oral administration of APIs. In the same study, THCPSi nanoparticles were dosed also via the subcutaneous and intravenous routes. The subcutaneously injected particles remained intact under the skin for at least 4 h. Accumulation in liver and spleen was detected after the intravenous administration. The same observation was achieved in a study where the effects of 1-2 μm PSi materials with positive and negative surface charges after single and multiple intravenous administrations to mice were followed (Tanaka et al., 2010a). Accumulation in kidney, heart, lung and brain was excluded and no significant changes were detected in the liver and spleen functions despite the particles' accumulation. In addition, neither signs of obvious changes in blood chemistry nor immunoreactivity, abnormal behavior or other clinical symptoms were detected, which support safe intravenous administration of the studied PSi particles to mice. Similar results with regard to safety issues were also obtained by Tanaka and co-workers (Tanaka et al., 2010b), although the degradation kinetics of PSi with positive surface charge from liver and spleen was considered different. During the three week study, the amount of silicon in the spleen decreased faster and was totally cleared, while there was still 25% of the original PSi amount remaining in the liver at the end of the study. Another report demonstrated the full clearance after four weeks of luminescent PSi nanoparticles (~126 nm) initially accumulated in liver and spleen (Park et al., 2009). *In vivo* the silicon is considered to degrade into silicic acid which is then excreted in the urine (Reffitt et al., 1999; Park et al., 2009). No significant toxicity was observed in the abovemetioned studies relative to animal body weight changes or histopathological issues.

Similarly to the early PSi studies, the investigation of the effects of mesoporous silica implants has also led to *in vivo* studies regarding the mesoporous silica safety. Favorable tissue response with good biocompatibility has been reported after subcutaneous, bone, and brain implantations of both ordered and non-ordered mesoporous silica materials without surface treatments (Kortesuo et al., 2000; Radin et al., 2005; López et al., 2006). Intraperitoneal administration of nonporous amorphous silica nanoparticles of on average 12 nm induced oxidative stress and inflammatory reactions in mice (Park and Park, 2009). Part of the injected particles remained at the injection site and part of them were delivered to other tissues via the blood stream. The administration route appears to be an important factor in mesoporous silica toxicity. When mesoporous silica materials between ~150 nm and ~4 μm were injected intramuscularly or subcutaneously to rats, no toxicity in addition to some reversible inflammation reactions was observed (Hudson et al., 2008). In this case, the amount of subcutaneously injected silica particles decreased progressively during three months, whereas the particles disappeared much faster from the intramuscular administration site. In addition, in the same study the particles were administered to mice via intraperitoneal, intravenous and subcutaneous routes (*e.g.* 100-150 nm particles; doses of 30, 6 and 30 mg, respectively). Again, the biocompatibility at the subcutaneous region was acceptable while the other injection routes resulted in death or euthanasia of the animals. The clearance of the silica materials was faster at the intraperitoneal site leading to higher systemic doses of the mesoporous silica particles and the intravenous administration delivered the materials straight into the systemic circulation. Thus, the kinetics and systemic dose of the materials was considered to be the critical issue with

regard to the material toxicity. The cause of death of the animals was not clear, but pulmonary embolism and/or thrombosis were suggested as possible causes.

Surface functionalization can be utilized to increase the circulation time of nanoparticles in the body and to hide them from the body defense mechanisms (Moghimi and Szebeni, 2003). Tetraethylene glycol functionalized mesoporous silica has been shown to be nontoxic and nonimmunogenic after intranasal administration or intrapleural injection into mice (Blumen et al., 2007). The particles remained in the close vicinity of the administration site, lung and diaphragm. After intrapleural injection, the particles were also found in the spleen. The material was 1–2 μm in diameter and, thus, unlikely to penetrate the endothelial or blood–brain barrier, which was considered one reason for the low toxicity. The same particles were loaded with gadolinium and were administered intraperitoneally to rats without any negative effect on behavior or pathology (Steinbacher et al., 2010). Additionally, the same particle type has been studied as a drug delivery vehicle subcutaneously and intraperitoneally with no signs of systemic toxicity (Hillegass et al., 2011).

There are also several studies where mesoporous silica has been administered to animals without reported side effects (Hsiao et al., 2008; Kim et al., 2008; Liu et al., 2008; Wu et al., 2008; Taylor et al., 2008; Mellaerts et al., 2008b; Lee et al., 2009; Wang et al., 2011). To conclude, the studies where toxic effects have been reported, it appears that functionalization of the mesoporous silica materials is recommended for parenteral administrations, whereas oral administration has been regarded as safe (FDA, 1979, 2011).

2.3 Mesoporous materials in drug delivery

Mesoporous silicon/silica-based materials have been widely studied as drug delivery vehicles (Salonen et al., 2008; Anglin et al., 2008; Wang, 2009; Vallet-Regí, 2010). Since the dawn of their applications as carriers for biologically active molecules (Vallet-Regí et al., 2001; Foraker et al., 2003), the effects of various modifications of particle properties on the release of the loaded substances has been under intensive research – initially *in vitro* and recently also *in vivo*. These issues will be discussed in the following chapters, excluding applications in tissue engineering and biosensing (Avnir et al., 2006; Vallet-Regí, 2006).

2.3.1 Modifying the drug release rate with particle properties

Several studies have shown that different biologically active agents can be loaded and, subsequently, released from silicon/silica-based mesoporous particles. The studies have been performed with silica gels (Takeuchi et al., 2004; Smirnova et al., 2005; Miura et al., 2010; Planinsek et al., 2011), ordered mesoporous silica (Vallet-Regí et al., 2001; Charnay et al., 2004; Shen et al., 2009; Van Speybroeck et al., 2009; Thomas et al., 2010; Zhang et al., 2010) and PSi (Salonen et al., 2005; Wang et al., 2010; Bimbo et al., 2011). The dissolution of poorly soluble drugs from the particles is usually faster than that of bulk

APIs. However, when the solubility of the API is high, a delayed release can be achieved from the particles (Salonen et al., 2005). The fast dissolution from the particles is related to the confined space inside the pores that prevents long range ordering, thus preventing the crystallization of the loaded substances (Salonen et al., 2005; Azaïs et al., 2006). The stabilized amorphous form of the molecules improves the drug dissolution rate (Hancock and Parks, 2000). The loaded substances have been suggested to interact with the surfaces of the particles via hydrogen bonding (Vallet-Regí, 2010). This increases the surface area of the APIs as compared to their crystalline counterparts, further improving the drug dissolution rate (Planinsek et al., 2011).

The pore diameter of the particle is one important factor affecting the release rate of the loaded substance. It has been shown that even changes as small as parts of nanometers in the pore diameter can affect the release rate of ibuprofen from ordered mesoporous silica MCM-41 (Horcajada et al., 2004). Several other studies have compared the effect of the pore diameter on the drug release using particles with different pore properties and concluded that the drug release rate usually increases with increasing pore diameter (Andersson et al., 2004; Qu et al., 2006a; Cauda et al., 2009). A contradictory effect has been shown with amorphous silica gels with wide range of pore diameters (2-21 nm) due to drug entrapment (Yang et al., 1979; Kinnari et al., 2011). It must be kept in mind that the release rate is always a combination of the properties of the loaded substance and the particle. In addition to the controlled release applications that are discussed in the next chapter, differences in the surface chemistry of the particles affect the release rate in immediate release formulations, as well (Kinnari et al., 2011). The release of different-sized molecules from the same-sized pores is different and the pore diameter should be adapted according to the molecule size (Izquierdo-Barba et al., 2005). There has also been suggested a pore diameter limit for a certain molecule, after which increasing of the pore diameter does not have any major impact on the drug release rate (Mellaerts et al., 2007). On the other hand, increasing extensively the pore diameter resulted in crystallization of the drug inside the pores, thus leading to a slower drug release rate (Shen et al., 2011; Miura et al., 2011). The limit pore diameter for ibuprofen was shown to lie between 10 and 20 nm. An *in vitro* and *in vivo* study revealed an interesting phenomenon: the *in vitro* release of fenofibrate was faster with increased pore diameter, whereas largest *in vivo* absorption was achieved with the smallest particle pore diameters (Van Speybroeck et al., 2010a). It was proposed that the slower rate, at which the supersaturation of the drug in the intestine is created, favors the absorption of fenofibrate.

In addition to the pore size, the pore morphology can also be modified in order to control the release rate of the loaded substance. The particle size and shape affect the length of the pathway that a molecule needs to travel in order to be released. Vancomycin diffusion into spherical SBA-15 particles was less restrained than into corresponding fiber-like material (Cauda et al., 2008). This was due to the small number of pore openings in the fiber-like particles as compared to the spherical ones. The phenomenon outweighed even the pore size effects. The shorter channel length of the pore has also been shown to have stronger impact on the release rate of captopril from MCM-41 than the pore size (Qu et al., 2006a). Overall, a more tortuous diffusion route makes the deeper parts of the particle less accessible to the drug, leading to poorer loading efficiency and possibly

entrapment of the molecules inside the mesoporous material (Cauda et al., 2009). Tortuous pore structure can also be utilized for controlling the release of a drug; however the silica solubility also affects the drug release rate in long-lasting studies (Andersson et al., 2004). Several studies have shown that the release is faster from 3D interconnected pore systems (Qu et al., 2006b; Heikkilä et al., 2007a, 2007b). The reason is suggested to be the easier accessibility of the dissolution medium into the particles.

2.3.2 Controlled drug release

2.3.2.1 Surface functionalization

The internal surfaces of the pores can be functionalized with different organic modifications in order to control the release of the loaded substances from the carrier particles. The change in the surface properties affects the physicochemical interactions between the loaded substance and the particle surface. One option is to add hydrophobicity to the hydrophilic silanol groups of the particles by anchoring hydrocarbon chains on their surface. This kind of functionalization decreases the pore size and also the wettability of the particle surface by aqueous solutions (Doadrio et al., 2006). Adding hydrophobic octyl hydrocarbon moieties (C8) on the particle surfaces has been shown to decrease the release rate of hydrophobic antibiotic erythromycin from a cubic mesoporous silica template by a factor of nearly six, as compared with the non-functionalized calcined material (Izquierdo-Barba et al., 2005). Increasing the length of the hydrocarbon chain decreases the drug release rate (Doadrio et al., 2006). This was shown with calcined and octyltrimethoxysilane (C8) or octadecyltrimethoxysilane (C18) functionalized SBA-15 particles loaded with erythromycin. The effect was strongly dependent on the solvent used in the functionalizing process. Also, the surfaces of PSi can be modified with hydrocarbons. PSi functionalization with dodecene (C12) decreased the release rate of hydrophobic drug dexamethasone by a factor of almost 20 as compared to unmodified PSi (Anglin et al., 2004). The functionalization of the freshly etched pores resulted in rather small pore diameters for dexamethasone incorporation. Thus, in order to produce pores wide enough for the dexamethasone incorporation, the pores were widened before the dodecene treatment. In addition to straight hydrocarbon chains, also other organic moieties can be used in the surface functionalization. For example, the release of ibuprofen with an acidic –COOH group was studied from MCM-41 matrices functionalized with different organic groups (chloropropyl, phenyl, benzyl, mercaptopropyl, cyanopropyl and butyl) (Horcajada et al., 2006). In certain samples, a large part of the ibuprofen remained on the surfaces of the particles. However, it could be shown that the total ibuprofen release rate from the particles with polar functional groups was the slowest. Sustained release of an active peptide has also been shown from THCPSi microparticles (Kilpeläinen et al., 2011).

Another widely studied surface modification type is the amino-functionalization. The amino-group ($-NH_3^+$) provides a counterpart for ionic interaction with acidic molecules, for example, with ibuprofen's carboxyl-group ($-COO^-$). The amino-functionalization also

increases the hydrophobicity of the pore surface. The release is often slower from the amino-functionalized particles (Manzano et al., 2008; Contessotto et al., 2009); however, the downside of the strong interaction between the particle surface and the loaded substance is the possible partial retention of the loaded molecules inside the particles (Nieto et al., 2008). The amount of positive ammonium groups affected the loading and release of anionic sulfasalazine from functionalized silica surfaces (Lee et al., 2008). Below neutral pH, the positive charge of the amino-groups attracted the anionic drug inside the pores. At neutral pH the unreacted surface of silanol groups were deprotonated resulting in electrostatic repulsion of the anionic drug, which in turn does not favor its presence inside the pores. Thus, the release and loading of the drug were shown to be pH-sensitive. In order to achieve the most effective loading degree, the phenomenon of opposite charges attracting each other can be utilized in drug loading and the surface treatment can be selected according to the substance that is intented to be loaded into the particles (Tasciotti et al., 2008). The method of functionalization is also critical for the drug release rate. Calcination of the material before treatment with aminopropyltrimethoxysilane produced particles where most of the functional groups were located inside the pores (Muñoz et al., 2003; Song et al., 2005). This resulted in denser packing of ibuprofen inside the pores and slower release of ibuprofen from those particles as compared with the non-calcined yet amino-functionalized particles. One challenge remaining in many surface-modified sustained release silicas is the initial burst release of the surface-bound drug (Nieto et al., 2008; Popovici et al., 2011). Similar sustained release results have been obtained with amino-functionalized SBA-15 particles covalently grafted with rhodamine B, which functions simultaneously as the source of positive surface charge, as well as in red fluorescent emission to enable further studies with cells (He et al., 2010).

2.3.2.2 Stimuli-responsive methods

Stimuli-responsive methods have been developed in order to achieve targeted release where the premature leakage of the loaded substance is minimized. Changes in human body environment, such as pH, temperature or sugar concentrations, can be utilized when stimuli-responsive systems are developed. Some of the triggers that have been used to release the drug from the particles are not applicable in human body; however, they are briefly described here.

pH-Responsive systems are well-known in traditional pharmaceutical formulations where pH-sensitive polymers are used to modify the release rate of a drug in the GI-tract. The method has also been proved functional with polymer-coated drug-loaded silica particles and tablets (Ohta et al., 2005; Xu et al., 2009). A more sophisticated method to achieve pH-controlled drug release is by tuning the orifices of the silica particles with pH-responsive molecules. This can be obtained, for example, by adsorbing polycations as gate-keepers next to the pore openings of carboxylic acid modified silica (Yang et al., 2005). The adsorption is based on ionic interactions. As the pH changes from neutral to acidic, the carboxylic acid is protonated and the polycation disconnected from the surface,

thus leaving the pores open for the loaded substance to be released. Coating with polyelectrolyte multilayers can also be used to control the molecule release from the pores either via pH or salt concentration changes of the release medium (Zhu et al., 2005). This method is also based on the ionic interactions between the coating materials and the silica surfaces. The pH responsivity of this system is similar to that of polycations, as the coating is incompact at low pH-values and closes the pore openings at high pH-values. Full blockage of the drug release is not achieved via these methods: a leakage of about 10% has been detected even at pH-values where the pores are closed. The polyelectrolyte multilayers are also sensitive to salt concentrations (Zhu et al., 2005). High ionic strength of 10 mM NaCl solution weakens the ionic interactions between the oppositely charged layers and leaves the pore openings unsealed. At lower salt concentration (0.5 mM) the electrostatic binding is not disturbed and the polyeletrolyte multilayers are able to cap the pore openings. An interesting idea was the use of gluconic acid-modified insulin proteins as caps in order to encapsulate cyclic adenosine monophosphate that induces insulin secretion into boronic acid functionalized mesoporous silica (Zhao et al., 2009). The release could be triggered by saccharides, such as glucose, providing a potential application for the treatment of diabetes. Thermoresponsive polymer poly(N-isopropylacrylamide) has also been incorporated into the silica structure to form hybrid materials (Fu et al., 2007). The polymer changes its molecular chain conformation from packed to loose when the temperature rises from room temperature to body temperature. This structural change in the hybrid particles triggers the release of the loaded substance. In addition, it has been shown that near-infrared radiation of mesoporous silica/gold nanorods nanocomposite increases the temperature of the system and, consequently, the release rate of the loaded substance (Al-Kady et al., 2011). The hyperthermia effect could be applied as a controlled drug release mechanism in, *e.g.* cancer therapy applications (Huang et al., 2006).

Controlled release of molecules from silica particles has also been achieved by methods that utilize various triggers, although they might be less straightforwardly applicable in human body. Coumarin derivatives that form dimers to block the pore openings and react reversibly to UV light with different wavelengths, have been successfully developed (Mal et al., 2003). When magnetic nanoparticles are used in pore capping or otherwise incorporated to the particles, they can be directed to a site of interest, from where the drug release is triggered (Giri et al., 2005; Huang et al., 2009). The separation of the cap can be induced, for example, by cell-produced antioxidants, such as dihydrolipoic acid, and also regulated by the trigger molecule concentration. Chemically removable caps include also surface-derivatized cadmium sulphide nanoparticles that can be removed from the pore openings by disulfide bond-reducing molecules (Lai et al., 2003). Moreover, in this application the release rate of the molecule can be controlled by the concentration of the trigger molecules. Other methods to control the release of molecules from silica particles have also been studied for, *e.g.* electronically responsive delivery (Batra et al., 2006) and ultrasound (Kim et al., 2006).

2.3.3 *In vivo* applications

In recent years, the interest in *in vivo* drug delivery of mesoporous silicon/silica-based materials has increased tremendously, and numerous research publications have emerged. The safety aspects were discussed earlier in this dissertation and, thus, *in vivo* studies regarding biocompatibility have been left out from this chapter.

An application that has proceeded the furthest in the development pipeline is pSivida's BrachySil^{TM} product – an intratumoral medical device composed of PSi containing beta-emitting phosphorous 32-P (Goh et al., 2007). This product has shown positive safety profiles in first-in-man and dose escalation studies in patients suffering of hepatocellular carcinoma and pancreatic cancer (Goh et al., 2007; pSivida Corp., 2011). Promising antitumoral responses have also been obtained. In another application, amino-functionalized PSi has been loaded with neutral nanoliposomes containing small interfering RNA (siRNA) targeted against an oncoprotein (EphA2), which is overexpressed in most cancers (Tanaka et al., 2010b). The formulation was administered once intravenously to mice and an effect of at least three weeks was obtained in the gene silencing. The treatment also decreased the tumor burden in the mice. The sustained release of the siRNA was associated with the electrostatic interactions between the positively charged PSi and the negatively charged cargo. PSi-studies in rat have shown that thermally oxidized, aminosilanized-PSi could be used as a delivery vehicle of cells to the ocular surface (Low et al., 2009). Pieces of the surface-modified PSi membranes were implanted in the rat eye with no major host reactions reported. Furthermore, THCPSi microparticles have also been successfully loaded with active food regulator peptides and, subsequently, administered subcutaneously to rats for food intake and heart rate or blood pressure studies (Kilpeläinen et al., 2009, 2011). In these studies the peptide activity remained after the release. The peptide release occurred in a sustained manner as shown by the prolonged effects of the peptides on the rat biological and behavioral responses.

Mesoporous silica has also been investigated as a vehicle for cancer therapy. Excellent tumor suppressing effect was shown with camptothecin-loaded mesoporous silica dosed intraperitoneally to breast cancer mice xenografts (Lu et al., 2010). Accumulation of the particles into the tumors was seen with the silica, with and without folic acid functionalization. There was no major difference in the amount of accumulation. In recent years, oral bioavailability of drugs administered utilizing mesoporous silica has been under intense investigation. Improved intestinal absorption of medicines from the silica-based formulations has been shown in rabbits and dogs (Mellaerts et al., 2008b; Miura et al., 2010). In rats, a precipitation inhibitor, hydroxypropylmethylcellulose (HPMC), combined to an SBA-15 formulation, improved the bioavailability of a poorly soluble drug by more than 60% when compared to a plain formulation of drug-loaded SBA-15 (Van Speybroeck et al., 2010b). However, it is not straightforward that a maximal supersaturation of a drug in the GI-tract always improves the drug bioavailability. When fenofibrate was administered to rats, a decrease in drug release rate was shown to favor higher plasma concentrations (Van Speybroeck et al., 2010a).

The *in vivo* research on mesoporous silicon/silica-based materials shows interesting future prospects. Rapid development of these materials towards clinical applications is

ongoing and it is anticipated that their full potential in medicinal products will be revealed in the future.

3 Aims of the study

The purpose of this work was to study the mesoporous materials in drug delivery and their use as carriers for poorly water soluble drugs. Mesoporous (PSi, $PSiO_2$) materials were compared with regard to drug loading, dissolution behavior, permeability, stability and tablet formulations. The specific aims were:

1. To evaluate the stability of the mesoporous materials and the loaded substance during storage.

2. To evaluate the utilizability of larger scale drug loading methods for mesoporous materials.

3. To analyze the effects of the pore size and the ordering of the pores on the loading and release of a poorly soluble drug.

4. To assess the importance of the PSi surface treatment on the release of a poorly soluble drug.

5. To study the relevance of the attained improved dissolution on the permeation rate of a poorly soluble drug across Caco-2 cell monolayers.

6. To study the functionality of the loaded mesoporous materials in pharmaceutical tablet formulations.

4 Experimental

Detailed descriptions of the methods, suppliers of the materials and the equipment used in this work can be found in the respective original publications (**I-IV**). Mesoporous silicon-based materials (**I, IV**) were produced in the Laboratory of Industrial Physics, Department of Physics and Astronomy, University of Turku, and ordered mesoporous silica materials (**II, III**) in the Laboratory of Industrial Chemistry, Process Chemistry Centre, Åbo Akademi.

4.1 Materials

4.1.1 Mesoporous particles (I-IV)

The PSi particles with various surface treatments were prepared from Si wafers (100), of p+-type with resistivity values of 0.015–0.025 Ωcm. The PSi was prepared by anodizing the wafers in a HF (38%)–ethanol (EtOH) mixture (HF:EtOH, 1:1). A current density of 50 mA/cm^2 was used to obtain a porosity of about 60% (**I**). Free-standing films were obtained by abruptly increasing the current density and ball milling of the films produced as-anodized PSi particles (**I**). The resulting powders were sieved with a 400 mesh sieve to obtain particle size fraction <38 µm for the experiments. Annealing in an inert atmosphere (N_2) was used to increase the pore diameter of the particles (**I**). Before the surface was carbonized to obtain TCPSi or annealed TCPSi (annTCPSi) (**I, IV**), the microparticles were treated with HF:EtOH (1:1, v/v) solution to replace the oxidized surface formed during milling with hydrogen termination. A two-step thermal carbonization process utilizing gaseous acetylene was used to form a stabilizing SiC-terminated surface on the particles (TCPSi and annTCPSi). The carbonization with phased acetylene treatments was performed at 500 °C followed by cooling down to room temperature, after which the temperature was raised to 820 °C without the acetylene flush (Salonen et al., 2005). Thermal oxidation does not require the previously described hydrogenating process with HF:EtOH solution. Instead, thermal oxidation was performed directly after the sieving and annealing processes at 300 °C (Salonen et al., 2005) to obtain TOPSi and annealed TOPSi (annTOPSi) particles, respectively (**I**).

Ordered mesoporous silicas, MCM-41 (**II, III**) and SBA-15 (**III**), were synthesized in an autoclave. The reagents used in the MCM-41 synthesis were fumed silica (SiO_2, 99.9%), tetramethylammonium silicate [$(CH_3)_4N(OH)\cdot 2SiO_2$, 99.99%], sodium silicate ($Na_2O_7Si_3$,SiO_2, 27%), cetyltrimethylammonium bromide [CTAB, $CH_3(CH_2)_{15}N(CH_3)_3Br$, 99%], and distilled water. Correspondingly, the reagents used in the SBA-15 synthesis were Pluronic P123 co-block polymer, HCl (33-40%), TEOS ($Si(OC_2H_5)_4$, 98%) and distilled water. A gel mixture was prepared for both syntheses and introduced in a Teflon cup, which was inserted in an autoclave. The autoclaves were kept in a large oven and the syntheses of MCM-41 and SBA-15 were performed at 100 °C. After the completion of the

syntheses, the autoclaves were removed from of the oven and the MCM-41 was quenched before the next step. The mesoporous silicas were filtered and washed with distilled water. The samples were dried at 110 °C (MCM-41) or at 100 °C (SBA-15) for 12 h. Finally the synthesized silicas were calcinated at 550 °C for 10 h (MCM-41) or at 500 °C for 7 h (SBA-15). The synthesized materials were gently milled in a ball mill and the resulting powders were sieved with a sieve shaker apparatus to obtain different particle size fractions for the experiments.

Non-ordered silica gel Syloid 244 FP EU (Grace Davison, Grace GmbH & Co. KG, Germany) was used as received (**III**).

4.1.2 Model compounds (I-IV)

Model drug compounds used in the studies were ibuprofen (**I**), indomethacin (IMC; **II, III**) and furosemide (**IV**). The structures and properties of these drugs are presented in Table 3.

Table 3. *Properties and structures of the model drug compounds (**I-IV**).*

Compound	Structure	Molecular weight	Water solubility[1] (µg/ml)	pK_a[1,2]	BCS class[3]	Publi-cation
Ibuprofen	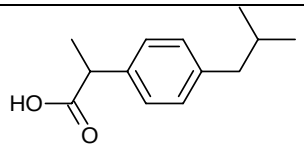	206.3	21	4.9	II	I
Indomethacin	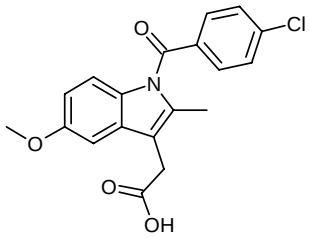	357.8	0.94	4.5	II	II, III
Furosemide	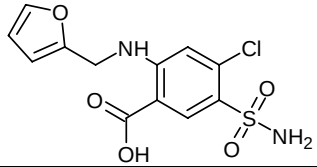	330.7	73	3.7 9.9	IV	IV

[1] Obtained from the Syracuse Research Corporation Physical Properties Database August 12th, 2011 (http://www.syrres.com/what-we-do/product.aspx?id=133).

[2] Furosemide pK_a was determined in **IV**.

[3] According to (Wu and Benet, 2005).

4.1.3 Cell culture (IV)

Human colon adenocarcinoma Caco-2 cells were obtained from American Type Culture Collection. The cells were grown in a medium consisting of Dulbecco's Modified Eagle Medium (4.5 g/l glucose) supplemented with 10% Fetal Bovine Serum (heat inactivated at 56 °C for 30 min), 1% Non Essential Amino Acids, 1% L-glutamine (200 mM), penicillin (100 IU/ml), and streptomycin (100 µg/ml). The cultures were maintained at 37 °C in an incubator at an atmosphere of 5% CO_2 and 95% relative humidity. The growth medium was changed three times a week during cell growth and differentiation. The cells were seeded at 6.8×10^4 cells/cm^2 onto polycarbonate filter membranes (pore size 0.4 µm, growth area 1.1 cm^2) in 12-Transwell inserts. Cells from passage numbers 31–42 were used in the experiments at ages ranging from 21 to 28 days.

4.1.4 Dissolution media and other chemicals (I-IV)

Buffered Hank's balanced salt solution (HBSS) was used as a medium in drug release studies (**I, IV**). Biological buffers HEPES (4-(2-Hydroxyethyl)piperazine-1-ethanesulfonic acid) or MES [2-(N-Morpholino)ethanesulfonic acid] at 10 mM concentration were used to buffer the HBSS. 0.2M HCl / 0.2 M KCl was the buffer used at pH 1.2 (**II**). In the experiments including a pH change from 1.2 to 6.8, 0.1 M HCl solution was used as the initial medium at pH 1.2, which was further raised to pH 6.8 by adding 0.2 M Na_3PO_4 solution (**II**). At pH 5.5, 0.1 M phosphate buffer was used (**III**).

Solvents used in the sample manufacture and analysis were EtOH (**I-IV**), phosphoric acid (**I-IV**), acetonitrile (**I, IV**), dichloromethane (**III**), methanol (**IV**), dimethylsulfoxide (DMSO) (**IV**) and octanol (**IV**). D-[^{14}C]mannitol solution was used to assess the Caco-2 monolayer integrity after the permeation studies. Excipients in tablet formulations (**III**) were Avicel PH 102 (microcrystalline cellulose), Ac–Di–Sol (croscarmellose sodium), Aerosil 200 (colloidal silica), Kollidon 30 (polyvinylpyrrolidone), Pharmatose 200 M (lactose monohydrate) and magnesium stearate.

4.2 Loading of mesoporous microparticles (I-IV)

Immersion loading method (I-IV)

In the immersion loading method the drug was first dissolved in an appropriate solvent at the following concentrations: ibuprofen (**I**) 800 mg/ml in EtOH, IMC 180 mg/ml and 250 mg/ml (**II**) or 17 mg/ml (**III**) in EtOH, and furosemide (**IV**) 600 mg/ml in DMSO. The loading was performed at room temperature, except for IMC loading in publication **II**, where heated EtOH at 68±2 °C was used as a solvent. The mesoporous particles were added and the suspension stirred for at least 1 h. After the loading, the suspension was filtered and the loaded particles were dried in an oven. The drying temperature varied between 60 and 120 °C depending on the solvent.

Rotavapor loading method (III)
IMC was dissolved in EtOH (9 mg/ml) at room temperature. The mesoporous particles were added and the suspension was shaken for at least 1.5 h. Next, the solvent was evaporated under reduced pressure in a water bath at 45-50 °C for 15 min using a rotavapor. The samples were dried under vacuum at room temperature.

Fluid bed loading method (III)
In the fluid bed loading method, the mesoporous silica particles were loaded using a MINI-Glatt fluidized bed. IMC was dissolved in EtOH (9 mg/ml). Syloid 244 FP EU or MCM-41 was added and the suspension was shaken for at least 1.5 h. The solvent was evaporated by spraying the suspension with the fluid bed machine. The atomizing air was heated to 90 °C to ensure fast evaporation of EtOH. The inlet air was fed to the system at room temperature to prevent mass from heating.

4.3 Analytical methods

4.3.1 Physical methods (I-IV)

Thermogravimetry was used with a temperature raise of 10 or 20 °C/min under N_2 or synthetic air gas flow, respectively (**I-IV**), to study the loading degree of the samples. Differential scanning calorimetry (DSC) was performed at heating rates of 2-20 °C/min under N_2 gas purge (**I-IV**) in order to detect crystalline portions of the drug on the surfaces of the particles after loading. Helium pycnometry was used to study drug loading in publications **I** and **IV**. The porous properties of the particles were studied utilizing N_2 ad/desorption (**I-IV**). The surface areas and pore characteristics were determined from the achieved data according to the BET (Brunauer-Emmett-Teller) and BJH (Barrett-Joyner-Halenda) methods. Fourier transform infrared spectroscopy (FTIR) was utilized to evaluate chemical changes in the samples, as well as possible residual solvents (**I**, **II** and **IV**). Information on ordered mesoporous silica structural properties and possible drug crystallinity was obtained by X-ray powder diffraction (XRPD; **II, III**). Raman surface mapping was used to characterize the solid form of IMC crystallized on the surface of the particles (**II**). Particle morphologies were evaluated from scanning electron microscopy (SEM) images (**II, III**) and a laser diffraction instrument equipped with a wet dispersion sampler was utilized to analyze particle size distributions (**II**).

4.3.2 Quantification of compounds (I-IV)

Concentrations of the model drug compounds in the drug release and permeation studies, and in the loading degree experiments were analyzed by high-performance liquid chromatography (HPLC). Descriptions of the HPLC-equipment used can be found in the

respective original publications (**I-IV**). HPLC-methods for the model compounds are shown in Table 4. For determination of [^{14}C]mannitol, 100 µl samples were mixed with 4 ml of a scintillation cocktail, and the [^{14}C]-activities were determined using a Liquid Scintillation Counter (**IV**).

Table 4. *HPLC methods for analyzing the model drug compound concentrations in the samples.*

Model compound	Aqueous phase	Organic phase	Flow rate (ml/min)	Retention time (min)	Wavelength (λ, nm)	Column
Ibuprofen (**I**)	0.03% phosphoric acid (50%)	acetonitrile (50%)	2	6.3	222	Bondapak C_{18}
Indomethacin (**II**, **III**)	0.2% phosphoric acid, pH 2.0 (40%)	acetonitrile (60%)	1.5	4.1	320	Luna 100Å C18
Furosemide (**IV**)	0.08 M phosphoric acid, pH 1.8 (60%)	acetonitrile (40%)	1.5	8.3	λ_{ex} = 233 nm λ_{em}=389 nm	Bondapak C_{18}

4.3.3 Determination of ionization and partitioning constants (IV)

The ionization constants (pK_a) and octanol–water partitioning coefficients (logP) were determined using a computerized Sirius GLpKa-potentiometric titrator at controlled temperature (25 ± 1 °C) and under argon flow. The results were processed using the Refinement Pro software. Apparent pK_a-values were determined in ionic strength adjusted methanol-water mixtures at several methanol concentrations and the aqueous pK_a-values were obtained through the Yasuda-Shedlovsky extrapolation procedure. Partitioning coefficients of unionized ($logP_{AH_2}$) and mono-anionic ($\log P_{AH^-}$) furosemide were obtained from titrations in the presence of octanol using three different octanol-water volume ratios. The log D (distribution coefficient) values were based on the determined logP values mentioned above, and the log-linear dependence is presented in Eq. (2):

$$\log D_{acid} = \log P - \log(1+10^{pH-pK_a}) \quad (2)$$

4.4 Tabletting (III)

The tablet masses were mixed manually. The tablets were compressed manually with an eccentric tablet machine using round flat-faced punches with a diameter of 5 mm. The target weight and crushing strength of the tablets were 50 mg and 60-80 N, respectively. The compression forces used for tabletting were 4.6 ± 2.4 kN. In addition, the thicknesses and the disintegration times of the tablets were measured according to the European Pharmacopoeia.

4.5 Drug release experiments (I-IV)

The utilized dissolution media in each study are described in chapter 4.1.4 (**I-IV**). Small volume dissolution studies were performed in the original publications **I** and **IV**. The experiments were performed utilizing Transwell cell culture inserts (polycarbonate membrane, pore size of 0.4 µm, 4.7 cm^2 area) and 6-well culture plates as donor and acceptor compartments, respectively. The loaded microparticles or the plain control drugs were weighed directly onto the filter inserts. The inserts were further placed into the well plates containing 2.75 ml of pre-warmed acceptor medium. Donor medium (1.5 ml) was added onto the filters and samples for HPLC analyses were collected at selected time intervals by moving the donor filter into the next receiver well with fresh medium. The studies were performed in an orbital shaker at 75 rpm and 37 °C under sink conditions.

The paddle dissolution method at 100 rpm described in the European Pharmacopoeia was used to study the drug dissolution in the original publications **II** and **III**. The volume of the media was 500 ml at 37 °C, and the studied substances were encapsulated in gelatin capsules (**II** and **III**) or studied as tablets (**III**) under sink conditions. During the drug release studies, 0.5 ml samples were collected at selected time intervals for quantification of the dissolving model drug compounds.

HPLC quantifications of the drugs loaded into the particles were performed by weighing 0.5-2 mg of particles in EtOH (**I** and **IV**) or 0.5-1 mg of particles in EtOH-water mixture (50:50) (**II** and **III**). The mixtures were vigorously stirred or shaken for few hours and the released drug amounts were then analyzed from the liquid fractions by HPLC.

4.6 Caco-2 permeability experiments (IV)

The permeability of furosemide across Caco-2 cell monolayers in an apical-to-basolateral (AP-BL) direction was studied at an apical pH of 5.5, 6.8 (pH-gradient conditions) and 7.4 (iso-pH), and basolateral pH of 7.4. Furosemide was introduced into the apical compartment either as pre-dissolved control solutions or as suspensions loaded into the TCPSi particles at the three pH values stated above. Additional control experiments of dispersed, unloaded furosemide were also performed under iso-pH conditions. Before the permeability experiments, the cell monolayers were first rinsed twice with HBSS (pH 7.4) and then equilibrated in the transport buffers under experimental conditions for 30 min. Transepithelial electrical resistance (TEER) was measured in order to confirm the integrity of the cell monolayers. Monolayers with TEER values above 250 Ωcm^2 were considered acceptable for the studies. At the beginning of the permeability experiment, the apical solution was changed to HBSS containing furosemide or furosemide loaded TCPSi particles (1.0–1.5 mg per monolayer). The suspensions were prepared immediately prior to the experiments. Basolateral samples were obtained at the selected time intervals by moving the inserts, containing the cell monolayers, to new receiver wells containing fresh HBSS (pH 7.4). All the permeability experiments were conducted at least in triplicate (n = 3–4).

Monolayer integrity was controlled after each permeability experiment by two methods. First, the cells were washed once with HBSS at the experimental pH and the TEER values were measured. In addition, the monolayer integrity was further assessed after the drug permeability tests with [^{14}C]mannitol. The apical washing solution was changed to a test solution with [^{14}C]mannitol solution (30 µl stock solution in 5 ml HBSS) at the experimental pH conditions. After 60 min, samples were withdrawn from the basolateral and apical compartments for activity measurements. Diffusion rates ≤0.5%/h were taken as an indication of normal monolayer integrity.

Cumulative amounts of the drugs transported across the Caco-2 cell monolayers were calculated from the concentrations measured in the receiver (BL) compartments. Apparent permeability coefficients, P_{app} (cm/s), were calculated based on Eq. (3):

$$P_{app} = \Delta Q/(\Delta t \cdot A \cdot C_0) \quad (3)$$

where $\Delta Q/\Delta t$ is the flux of the drug compound across the cell monolayers (µg/min), A (cm^2) is the surface area of the cell monolayer, and C_0 is the initial concentration (µg/ml) of the compound in the donor (AP) compartment. For the TCPSi experiments, the apparent permeability coefficients were estimated using C_0 values based on the complete dissolution of the full dose contained in the TCPSi particles. The dose was obtained from the analyses of the EtOH extracted samples (n = 3–4) taken from the TCPSi suspensions used in the permeation experiments.

5 Results and discussion

5.1 Characteristics of the studied mesoporous materials (I-IV)

The mesoporous carriers studied in this dissertation vary from each other in many physicochemical properties, some of which are compared in Figure 6. Most of the materials are hydrophilic, except as-anodized-PSi that is hydrophobic due to the hydrogen atoms on the surface. The three most obvious differences of the particles are the material itself, PSi or silica; the production method (Chapter 2); and the pore structure, ordered (MCM-41 and SBA-15) or less ordered (PSis and Syloid 244 FP EU). In addition, pore dimensions provide versatility to the materials despite the fact that they all belong to the class of mesoporous materials holding pore diameters between 2 and 50 nm (Rouquerol et al., 1994).

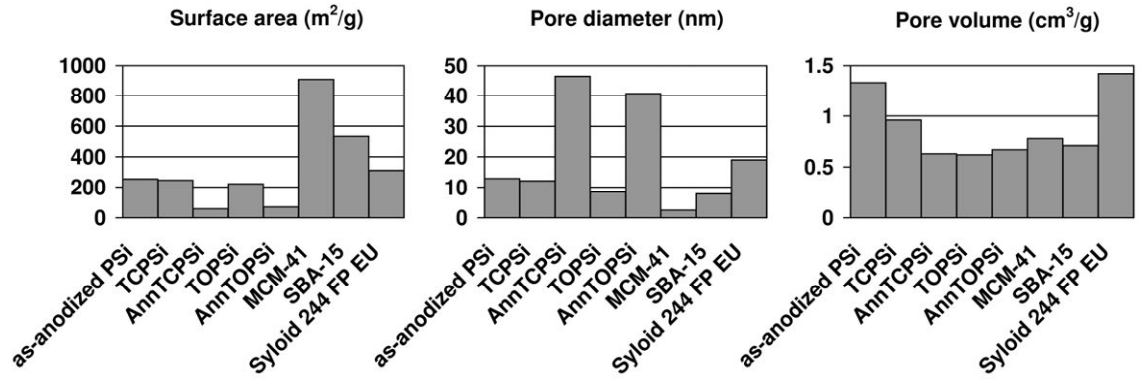

Figure 6. *Physical parameters of the studied mesoporous PSi and silica materials.*

The surface areas of the silica materials are notably larger than those of the silicon-based materials (Figure 6). This provides more potential for stabilizing the drug-surface interactions. Annealing of the as-anodized PSi widens the pores of the particles, which further decreases the surface area. At the same time, in the process of coarsening, some of the pores melt together and result in a smaller overall pore volume. Because the annealing is performed before the surface treatment, it does not have an effect on the hydrophilicity of the material. Surface treatment of the as-anodized PSi decreases the surface area slightly, but diminishes the pore volume more strongly. The higher pore volume provides more space for drug loading. On the other hand, when the pore diameter is wider, the carrier material no longer restricts the crystallization of the loaded substance, which in turn may have a negative impact on the drug dissolution rate. This possibility is anticipated mostly in the annealed PSi materials and silica gel Syloid 244 FP EU (Figure 6). The main difference in the studied PSi materials is their surface treatment (carbonization or oxidation) and the annealing effects. With regard to ordered mesoporous silicas, MCM-41 has narrower pores and larger surface area than SBA-15. The mesoporous silica materials have basically similar surfaces, but the number of silanol

groups/nm^2, α_{OH}, is generally higher in SBA-15 (2.8-5.3 OH/nm^2) than in MCM-41 (1.4-3.0 OH/nm^2) ordered silica materials; the value for conventional silica gel, 4.2-5.7 OH/nm^2, has been measured as the highest of these three silica materials (Zhuravlev, 1987; Zhao et al., 1997; Shenderovich et al., 2003; Kozlova and Kirik, 2010). However, the overall number of the silanol groups in a particle is compensated by the differences in surface area (Figure 6). The silanol groups may interact with the functional groups of the loaded substances and stabilize their physical state (Bahl and Bogner, 2006). The interactions may also protect the loaded substances from chemical degradation. These phenomena, in turn, may compensate for the effects on drug release derived from the differences in the porous properties of the materials, such as higher probability for a drug to crystallize in a wider pore.

5.2 Loading of the materials (I-IV)

Immersion loading has been the widely used method to load drugs into the mesoporous materials in laboratory scale (Vallet-Regí et al., 2001; Salonen et al., 2005; Heikkilä et al., 2007b). In the immersion loading method, the empty carrier particles are added into a high-concentrated drug solution, and the loaded particles are separated from the solution by filtration at the end of the process. The method was also applied in this dissertation (**I**, **II**, **IV**). In publication **III**, it was shown that the high concentration gradient from the loading solution is the key factor affecting the loading efficiency. In the immersion loading method, the high concentration of the loading solution is achieved, for example, by effective chemical solvents or heating (Salonen et al., 2005). Thus, the method requires excessive amounts of the drug, energy and chemicals, which reduces the economical efficiency of the process. In publication **III**, two new methods for drug loading were successfully employed and evaluated: rotavapor and fluid bed. High payloads (~25-40 w-%) of the studied drugs were achieved in all studies (**I-IV**), except for the immersion loading method without driving concentration gradient in **III**.

The rotavapor and fluid bed loading methods are based on the increasing driving drug concentration due to the evaporation of the loading solvent (**III**). In these methods, no excess drug is needed to achieve successful payloads in the particles. In the rotavapor loading method, the solvent evaporates relatively slowly and gives the molecules time to diffuse inside the particles – even from small pore orifices as shown in publication **III** with MCM-41 particles. Instead, in the fluid bed loading method the evaporation of the solvent occurs fast, as the suspension of the drug solution and the particles is sprayed into the product chamber. The particles are separated from the loading solution at the same time and the driving force of the high drug concentration is only apparent for a short time. This makes the loading of small-pore-sized particles with fluid bed more challenging, as there is a risk of drug crystallization onto the surface of the particles, as seen in publication **III** with MCM-41 particles. It has also been shown that the pore morphology affects the loading efficiency (Cauda et al., 2008, 2009). Tortuous pore morphology makes the deeper parts of the particle less accessible for the drug. In publication **III**, the loading of Syloid 244 FP EU was successful in fluid bed despite its non-ordered pore structure.

This was due to the relatively large pore diameter and small particle size that compensated for the morphology effect.

5.3 Stability of the loaded particles (I, II)

The stability of the loaded drug and the drug release from the particles were studied after storage at 30 °C under 56% relative humidity for 3 months (**I**, **II**). The stability studies were performed with ibuprofen-loaded as-anodized PSi, TCPSi and TOPSi, in addition to the annealed counterparts of the two latter particles (**I**), and the IMC-loaded ordered mesoporous silicas MCM-41 and SBA-15 (**II**).

TOPSi and TCPSi particles proved to be good carriers for ibuprofen, as only negligible changes in the loading degrees of the materials were detected after the stressing conditions (**I**) (Table 5). The drug release rates were slightly slower after stressing; however, the effect of improved drug dissolution was still clearly present for the drug-loaded particles. The as-anodized PSi was oxidized during storage, as shown by the FTIR analyses of the particles after extraction of the loaded ibuprofen. The oxidation with the as-anodized PSi has been detected also elsewhere (Salonen et al., 1997). Chemical changes in the as-anodized PSi material were observed also with HPLC, where the ibuprofen loading degree was decreased from 40.7 to 29.7% during storage (Table 5). DSC showed some crystallization of ibuprofen on the surface of TOPSi particles and also a decrease in drug load was detected with HPLC after storage (Table 5), probably due to the chemical reactivity of TOPSi (Salonen et al., 2008). Overall, in this study it was shown that the surface stabilization of the PSi is essential and should be optimized when these materials are utilized as drug carriers.

Table 5. *Extent of drug loading (w-%) determined by HPLC from different mesoporous silicon (**I**) and silica (**II**) materials before and after storage for 3 months at 30 °C / 56% relative humidity (mean, n = 2-5). Two different particle size fractions of MCM-41 and SBA-15 were studied in publication **II** denoted as (1) and (2).*

Material	Drug	Before storage	After storage
as-anodized PSi	ibuprofen	40.7	29.7
TCPSi	ibuprofen	30.3	31.9
annTCPSi	ibuprofen	38.9	38.1
TOPSi	ibuprofen	37.6	31.6
annTOPSi	ibuprofen	28.8	29.9
MCM-41 (1)	indomethacin	30.9	22.8
MCM-41 (2)	indomethacin	31.9	21.7
SBA-15 (1)	indomethacin	29.5	32.7
SBA-15 (2)	indomethacin	40.9	38.5

In the studies with two size fractions of ordered mesoporous silica MCM-41 and SBA-15 microparticles, no evidence of physical changes were observed after stressing (**II**).

However, the HPLC drug loading degree results showed a decrease of the drug amount in the MCM-41 materials, while no major changes were observed in the drug loading degrees of SBA-15 (Table 5). Degradation of IMC inside the particles was corroborated by the HPLC chromatograms, where IMC degradation peaks at relative retention times (RRT) of 0.7 and 1.8 were seen after the stressing. As the HPLC method was not optimized for the degradation product quantification, the evaluations were made based on the relative peak areas between the possible IMC degradation product peaks and the corresponding IMC peak. These values were then compared between the non-stressed and stressed samples. Additional peaks were observed in the samples extracted from both the particle types, with lesser extent in SBA-15 than MCM-41 –derived samples, presenting representative relative peak area values of 2.67 and 9.82, respectively, as compared to the corresponding non-stressed samples with reference value of 1.00. The differences between MCM-41 and SBA-15 in the stabilization of IMC may derive from the number of silanol groups on the particle surfaces. As discussed in chapter 5.1, the number of silanol groups per surface area on the SBA-15 surface is higher that on the MCM-41 surface. Those groups are able to interact with carboxyl and benzoyl carbonyl groups of IMC, and contribute to the stabilizing of the amorphous form (Bahl and Bogner, 2006). This stabilizing effect may also explain the better chemical stability of IMC in SBA-15 than in MCM-41. The release profiles of IMC from the silica particles also remained similar after stressing. However, the drug release was somewhat slower than before stressing. To conclude, it was demonstrated that the silica materials are highly appropriate carriers for the poorly soluble drug IMC. In the future, the interactions of the loaded substance and the surface of the silica materials should be carefully evaluated and the chemical stability of the materials followed over time.

5.4 Tablet formulation (III)

In order to develop industrially feasible products, the mesoporous drug carriers need to be further formulated into applicable dosage forms. Capsules used in drug release studies are one alternative, however, tablets are often considered the preferred option in oral drug delivery. Tablets were compressed from the mesoporous silica materials, MCM-41 and Syloid 244 FP EU, to show their applicability in drug formulations. The tablet formulations were composed of two diluents, a binder, a disintegrant, a glidant and a lubricant in typical pharmaceutical amounts, in addition to the 25% of the loaded silica particles in the compositions. Tablets were successfully compressed from both particle types. The disintegration times of the tablets met the requirements of the European Pharmacopoeia, however, disintegration of the Syloid 244 FP EU tablets was remarkably slower (on average 6.8-11.6 min) than that of the MCM-41 tablets (on average 0.8-3.5 min). This was assumed to derive from the small particle size of Syloid 244 FP EU resulting in a denser packing of the tablet components, which in turn may have caused slower wetting and disintegration of the tablets.

XRPD patterns of gently crushed MCM-41-based tablets were used to evaluate the mechanical stability of the mesoporous structures after tabletting. The typical peaks of

MCM-41 (Beck et al., 1992) at approximately 2.5° and between 4° and 5° were observed also after the tabletting, thus supporting the idea that the mesopore structure of the particles was preserved. In addition, excipients and IMC were extracted from the Syloid 244 FP EU and MCM-41 samples as effectively as possible, and the N_2 isotherms of the samples were analyzed. The detected BET surface areas and the shapes of the hysteresis loops of the N_2 sorption isotherms indicated no major changes in the mesoporosity of either material. The results indicated that IMC-loaded mesoporous silica materials can be successfully formulated into tablets without compromising their characteristic structural properties.

5.5 Drug release studies (I-IV)

Loading of the studied drugs, ibuprofen, indomethacin and furosemide, into mesoporous particles improved the dissolution of the drug as compared to bulk material in all the studies (**I-IV**). Different properties of the mesoporous materials affecting the drug release rate were studied in publication **I** (surface treatment of PSi and pore size), publication **II** (pore diameter of silica), and publication **III** (order of pores, pore diameter and particle size). In addition, the IMC release was evaluated after tabletting of the drug-loaded mesoporous materials, MCM-41 and Syloid 244 FP EU.

Drug release from the surface-treated PSi is a complex phenomenon and it is affected by the combined effects of the pore size and surface chemistry (**I**). Hydrophilic surfaces of TOPSi and TCPSi were clearly beneficial for particle wetting and drug release when compared to the as-anodized, hydrophobic particles. Generally, a wider pore diameter contributes to a faster release of the loaded substance (Qu et al., 2006a; Cauda et al., 2009). As the ibuprofen release from TCPSi was faster than from TOPSi or as-anodized particles, one would assume that the release would have been even faster from the annTCPSi with the same surface treatment but wider pores. However, this was not observed in publication **I**; instead, the release from annTCPSi was remarkably slower (Figure 7). On the other hand, the release from annTOPSi was slightly faster than from TOPSi (Figure 7). This contradiction between the results could be due to differences in the crystalline fractions of ibuprofen on particle surfaces. If the crystalline fraction in annTCPSi would have been markedly larger than in TCPSi it could have exceeded the effects of the pore size. However, the crystalline fractions of the annealed materials could not be detected due to unclear melting peaks and thus this interpretation remained as a hypothesis.

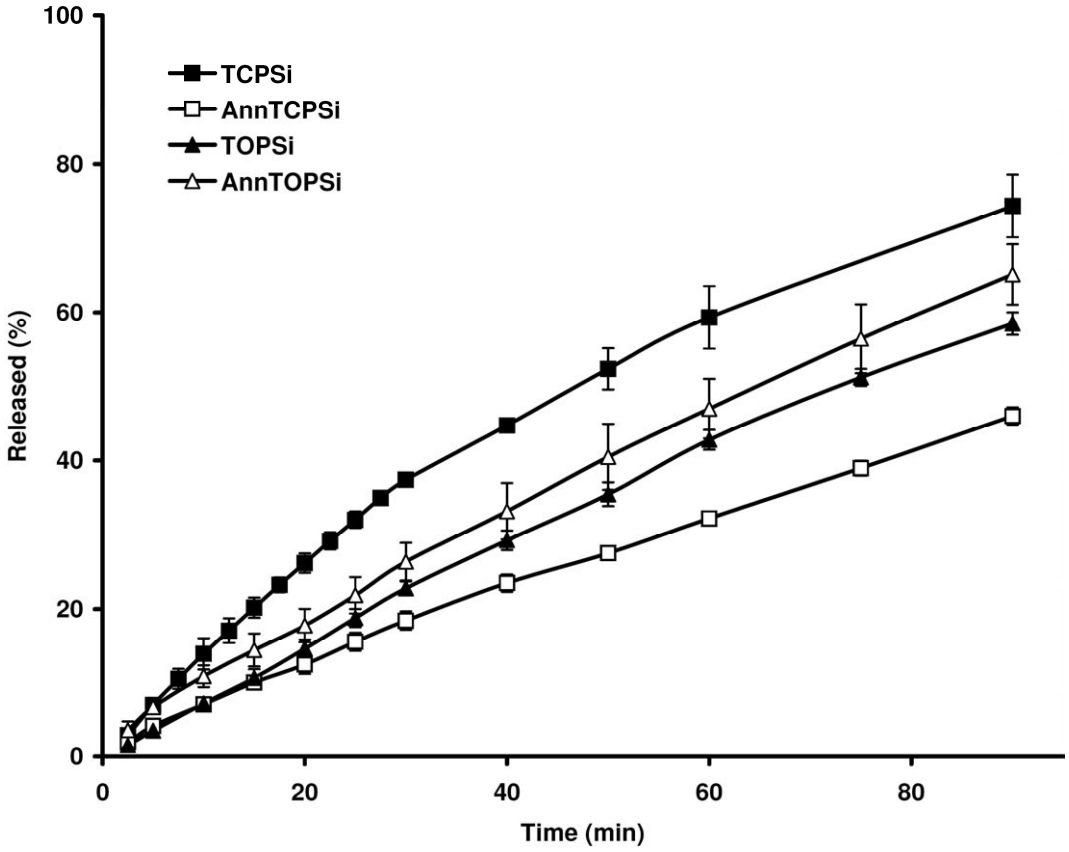

Figure 7. *Release profiles of ibuprofen from PSi particles with different surface treatments and pore diameters (n = 3-6, mean ± SD). Dissolution medium was HBSS (pH 5.5) at 37 °C.*

The release of IMC from MCM-41 mesoporous silica particles encapsulated into gelatin capsules was studied at pH 1.2 (**II**) and pH 5.5 (**III**) in 500 ml of relevant buffer at 37 °C. The effect of changing the pH from 1.2 to 6.8 during the IMC release from MCM-41 was studied in publication **II**. In addition, the effect of tabletting excipients in a capsule and tabletting process on the IMC release rate was studied in publication **III**. Bulk IMC dissolution was measured as a reference (publications **II** and **III**). These results are combined in Figure 8. The loading degree of the compared mesoporous materials was relatively similar: 31.9% in publication **II** and 24.4% in publication **III**. Interestingly, changing the pH from 1.2 to 5.5 did not affect the release rate of IMC from the MCM-41 particles, as shown by the overlapping release curves in Figure 8. Despite the fact that all the experiments were performed under sink conditions, the drug release at pH values of 1.2 and 5.5 was slow after the initial (burst) release phase, as observed elsewhere (Andersson et al., 2004; Qu et al., 2006a). However, close to complete IMC release was attained when the pH was changed from 1.2 to 6.8 (**II**). Similar pH effect was reported with ibuprofen-loaded MCM-41 (Charnay et al., 2004). IMC has an ionization constant of 4.5, and as a weak acid it is partly present in unionized form at pH 5.5, but almost fully ionized at pH 6.8 (Avdeef, 2001). Thus, at pH 6.8 the ionized form is favored in solution,

whereas at lower pH values the interior of the particles may provide more favorable environment for IMC. This could explain the observed differences in IMC release from the MCM-41 particles at different pH-values. Surprisingly, when common tabletting excipients were added to the MCM-41 capsule (**III**), dissolution of IMC was remarkably improved at pH 5.5 (Figure 8). In comparison, the effect of excipients on bulk IMC was clear, but still minor. Such a major effect of excipients on the release rate of a drug loaded into the mesoporous silica has not been reported earlier. Mesoporous silica SBA-15 itself diminished itraconazole supersaturation, and the phenomenon was partially compensated by precipitation inhibitors, such as HPMC (Van Speybroeck et al., 2010b). A similar mechanism may have provided synergy between the excipients and the fast release of IMC from the ordered mesoporous silica formulations in this study. In this study it was demonstrated that the improved IMC dissolution from the MCM-41 was maintained after tabletting (Figure 8).

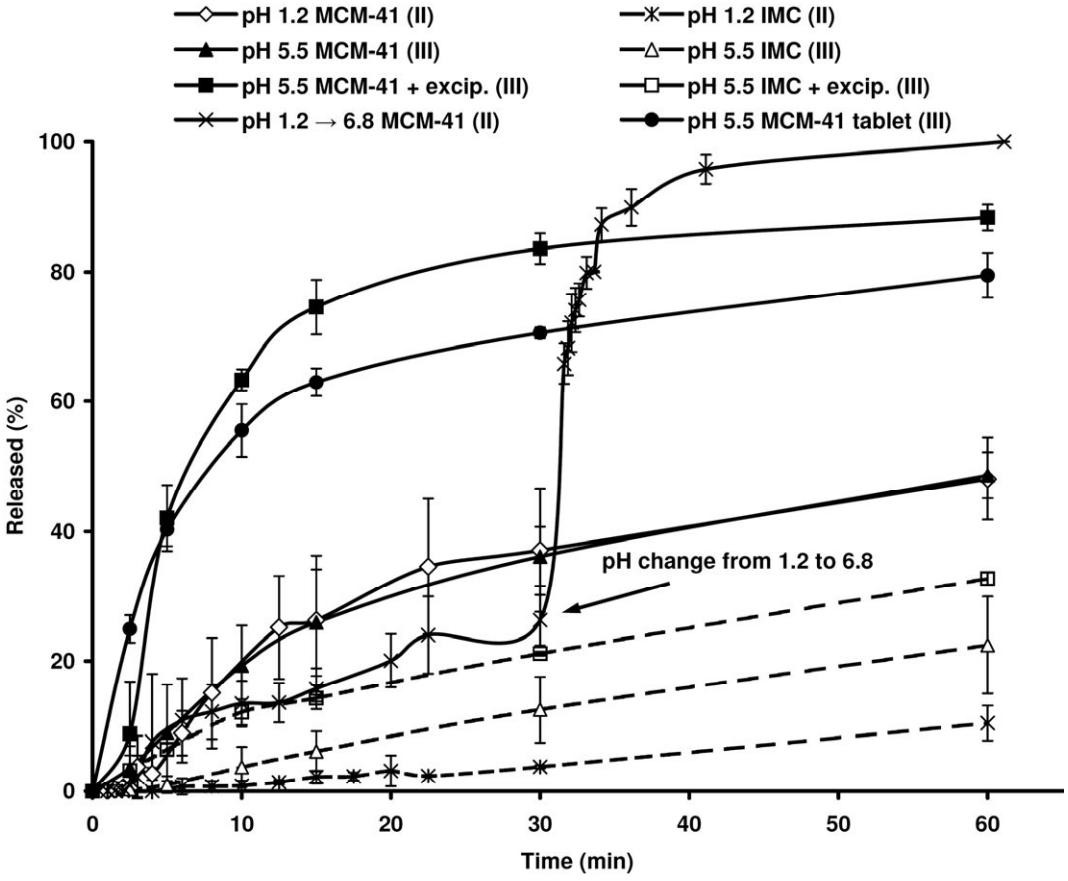

Figure 8. *Release profiles of IMC from encapsulated or tabletted MCM-41 particles (solid lines, n = 3-4, mean ± SD). Dissolution medium was 0.2 M HCl / 0.2 M KCl (pH 1.2), phosphate buffer (pH 5.5) or 0.1 M HCl at pH 1.2 which was further raised to pH 6.8 by adding 0.2 M Na_3PO_4 (pH change) at 37 °C. Bulk IMC is included as a reference (dashed lines).*

The porous properties of silica were further assessed in publications **II** and **III**. The IMC release from MCM-41 (**II**, **III**), SBA-15 (**II**) and Syloid 244 FP EU (**III**) were

evaluated at pH 1.2 in publication **II** and at pH 5.5 in publication **III**, and the results are combined in Figure 9 for better comparison. The release was the slowest from the particles with the smallest pore diameter, MCM-41, and became faster with increasing pore diameter (Figures 6 and 9). In addition, the smaller the particle size is, the faster the drug molecule diffuses out of the particle (Qu et al., 2006a; Cauda et al., 2008). Thus, the smaller particle size of Syloid 244 FP EU (2.5-3.7 µm), as compared to that of the studied ordered mesoporous silicas (< 125 µm), favored the faster IMC release from the particles (Fig. 9).

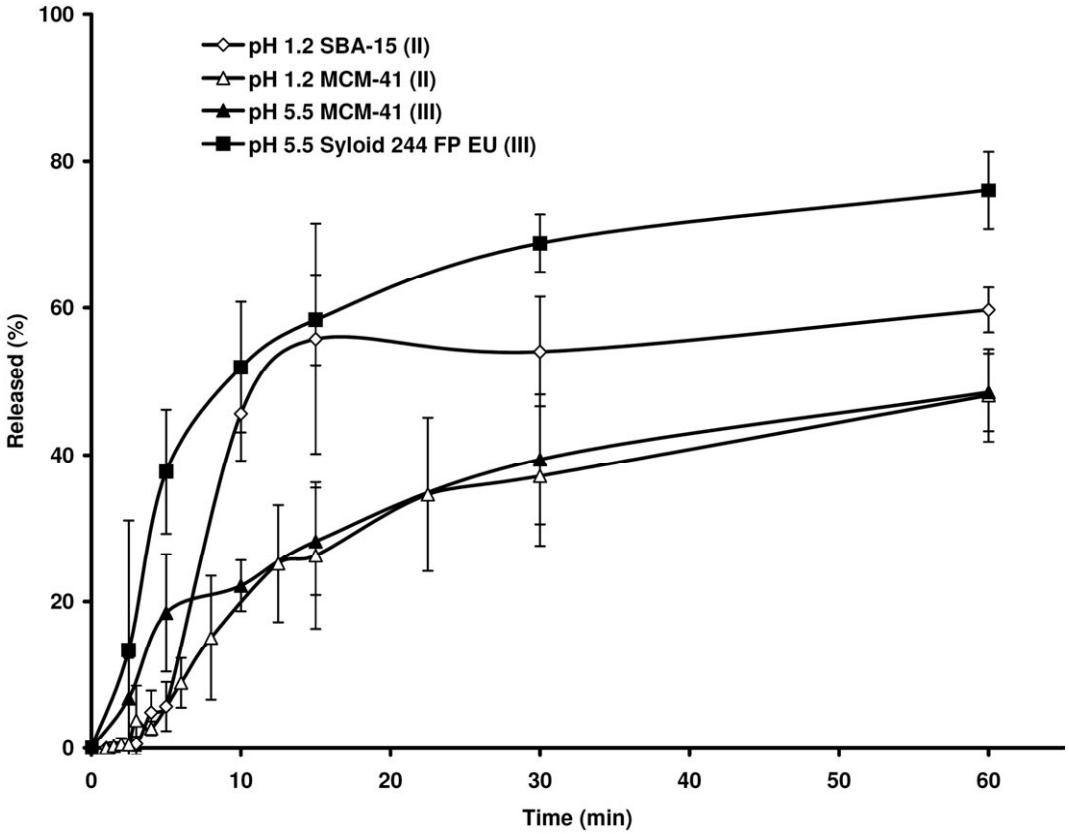

Figure 9. *Effect of the pore properties on the IMC release from mesoporous silica at different pH values (n = 3-4, mean ± SD). Dissolution medium was 0.2 M HCl / 0.2 M KCl (pH 1.2) or phosphate buffer (pH 5.5) at 37°C.*

5.6 Permeation (IV)

Furosemide, a poorly soluble and permeable drug, was loaded into TCPSi particles and the drug absorption was evaluated in Caco-2 permeability studies. Drug permeability was improved from the TCPSi particles as compared to pre-dissolved solutions at all the pH-values studied. The improved furosemide dissolution from the TCPSi particles provided higher local concentrations of the drug for absorption through the cell monolayers than from the plain furosemide solutions, especially at pH 5.5 where the poor solubility of

furosemide limited the drug concentration in the control solution. The Caco-2 monolayer integrity was not compromised during the permeability experiments.

A clear pH effect was also observed in the studies. The determined pK_a values for furosemide are pK_{a1} 3.70 ± 0.04 and pK_{a2} 9.93 ± 0.09. The logD values were estimated according to the Eq. (2) as $logD_{pH5.5}$ = 0.54 and $logD_{pH7.4}$ = 0.03. Due to the high acidic strength, the lipophilicity of furosemide decreases with increasing pH, which does not favor absorption. This explains the pH effect in the permeability results of furosemide. Also, the pH gradient from 5.5 to 7.4 across the cell monolayers provided favorable conditions for drug permeation via enhanced sink conditions. The overall permeability of furosemide was at the highest when loaded in the particles at apical pH 5.5 (P_{app} = 18.0 ± 1.3 $\times 10^{-6}$ cm/s, Table 6), and diminished with increasing pH. The effect was more pronounced with solutions, where the apparent permeability was dramatically decreased from 12.2 to 0.93 × 10^{-6} cm/s, due to the change of the apical pH from 5.5 to 6.8. Probably, due to the dissolution improving effects of TCPSi the change in P_{app} was less steep, despite clear, in the microparticle studies (Table 6). The highest relative increase (4.6 times) in the drug permeability from drug-loaded TCPSi compared to the drug solution was detected at apical pH 7.4, where the drug solution concentration was high, but the drug permeability from the solution was the poorest. Even the small increase in drug solubility provided by TCPSi formulation seemed to have a distinctive effect on the permeation of furosemide.

Table 6. *Apparent permeabilities ($P_{app} \times 10^{-6}$ cm/s; means ± SD) of furosemide across Caco-2 monolayers from pre-dissolved furosemide (control solutions) and estimates for furosemide-loaded TCPSi microparticles.*

Apical pH	**Control solutions**		**TCPSi-loaded**[1]		**P_{app} TCPSi / solution**
	Conc (µg/ml)	**$P_{app} \times 10^{-6}$ cm/s**	**Conc (µg/ml)**	**$P_{app} \times 10^{-6}$ cm/s**	
pH 5.5	150	12.2 ± 1.0	520	18.0 ± 1.3	1.5
pH 6.8	600	0.93 ± 0.38	840	4.1 ± 0.5	4.4
pH 7.4	650	0.30 ± 0.01	670	1.38 ± 0.05	4.6

[1] The apparent permeability coefficients were estimated using C_0 values based on the complete dissolution of the full dose contained in the TCPSi particles.

6 Conclusions

In this study several silicon- and silica-based mesoporous materials were tested and evaluated for drug delivery applications. The results clearly indicate that their performance as pharmaceutical carriers for poorly water soluble drugs is promising. The main conclusions drawn from the results are:

- The ibuprofen, indomethacin and furosemide release profiles from the loaded mesoporous materials were improved as compared to those of the respective bulk drugs before and after the storage.

- Rotavapor and fluid bed equipment was successfully employed in the loading of indomethacin into the mesoporous silica. The loading was efficient and did not require excessive amounts of the drug.

- Several aspects affect the loading efficiency and the release rate of ibuprofen and indomethacin from the mesoporous silicon and silica. A wider pore diameter facilitated easier access and release of indomethacin into and out of the mesoporous silica particles.

- The surface treatment of PSi is important for stabilizing the system. Different chemical treatments changed the hydrophilicity/hydrophobicity of the porous silicon materials and also the potential interactions between the loaded drug and the particles.

- The permeability of furosemide across Caco-2 monolayers was improved by loading of the drug into thermally carbonized PSi (TCPSi).

- It is possible to compress indomethacin-loaded mesoporous silica materials into tablets without compromising the improved drug release or the characteristic structural properties of the particles.

The mesoporous silicon- and silica-based materials provide a versatile platform for drug delivery. Their ability to stabilize the non-ordered form of loaded compounds is a promising feature with regard to oral drug delivery of poorly water soluble drugs. On the other hand, surface modifications open new possibilities for controlled drug release and targeting drug delivery (*e.g.* in cancer therapy). Positive safety profiles of mesoporous silicon- and silica-based materials have been reported after oral administration, which encourages the continuation of *in vivo* drug delivery studies with these materials in the future.

References

Adhiyaman, R., Basu, S.K., 2006. Crystal modification of dipyridamole using different solvents and crystallization conditions. Int. J. Pharm. 321, 27-34.

Ainslie, K.M., Tao, S.L., Popat, K.C., Desai, T.A., 2008. In vitro immunogenicity of silicon-based micro- and nanostructured surfaces. ACS Nano 2, 1076-1084.

Al-Kady, A.S., Gaber, M., Hussein, M.M., Ebeid, E.-Z.M., 2011. Nanostructure-loaded mesoporous silica for controlled release of coumarin derivatives: A novel testing of the hyperthermia effect. Eur. J. Pharm. Biopharm. 77, 66-74.

Amidon, G.L., Lennernäs, H., Shah, V.P., Crison, J.R., 1995. A theoretical basis for a biopharmaceutic drug classification: The correlation of in vitro drug product dissolution and in vivo bioavailability. Pharm. Res. 12, 413-420.

Anderson, S.H.C., Elliott, H., Wallis, D.J., Canham, L.T., Powell, J.J., 2003. Dissolution of different forms of partially porous silicon wafers under simulated physiological conditions. Phys. Status Solidi A 197, 331-335.

Andersson, J., Rosenholm, J., Areva, S., Linden, M., 2004. Influences of material characteristics on ibuprofen drug loading and release profiles from ordered micro- and mesoporous silica matrices. Chem. Mater. 16, 4160-4167.

Andrews, G.P., 2007. Advances in solid dosage form manufacturing technology. Philos. Transact. A Math. Phys. Eng. Sci. 365, 2935 -2949.

Andronis, V., Yoshioka, M., Zografi, G., 1997. Effects of sorbed water on the crystallization of indomethacin from the amorphous state. J. Pharm. Sci. 86, 346-351.

Anglin, E.J., Cheng, L., Freeman, W.R., Sailor, M.J., 2008. Porous silicon in drug delivery devices and materials. Adv. Drug Delivery Rev. 60, 1266-1277.

Anglin, E.J., Schwartz, M.P., Ng, V.P., Perelman, L.A., Sailor, M.J., 2004. Engineering the chemistry and nanostructure of porous silicon Fabry-Pérot films for loading and release of a steroid. Langmuir 20, 11264-11269.

Artursson, P., Lindmark, T., Davis, S.S., Illum, L., 1994. Effect of chitosan on the permeability of monolayers of intestinal epithelial cells (Caco-2). Pharm. Res. 11, 1358-1361.

Aulton, M.E. (ed.), 2002. Pharmaceutics: The science of dosage form design. Churchill Livingstone, Edinburgh, United Kingdom.

Avdeef, A., 2001. Physicochemical profiling (solubility, permeability and charge state). Curr. Top. Med. Chem. 1, 277-351.

Avnir, D., Coradin, T., Lev, O., Livage, J., 2006. Recent bio-applications of sol–gel materials. J. Mater. Chem. 16, 1013-1030.

Azaïs, T., Tourné-Péteilh, C., Aussenac, F., Baccile, N., Coelho, C., Devoisselle, J.-M., Babonneau, F., 2006. Solid-state NMR study of ibuprofen confined in MCM-41 material. Chem. Mater. 18, 6382-6390.

Bahl, D., Bogner, R.H., 2006. Amorphization of indomethacin by co-grinding with Neusilin US2: Amorphization kinetics, physical stability and mechanism. Pharm. Res. 23, 2317-2325.

Bansal, A., Li, X., Lauermann, I., Lewis, N.S., Yi, S.I., Weinberg, W.H., 1996. Alkylation of Si surfaces using a two-step halogenation/Grignard route. J. Am. Chem. Soc. 118, 7225-7226.

Bashiri-Shahroodi, A., Nassab, P.R., Szabó-Révész, P., Rajkó, R., 2008. Preparation of a solid dispersion by a dropping method to improve the rate of dissolution of meloxicam. Drug Dev. Ind. Pharm. 34, 781-788.

Batra, I., Coffer, J.L., Canham, L.T., 2006. Electronically-responsive delivery from a calcified mesoporous silicon structure. Biomed. Microdevices 8, 93-97.

Beck, J.S., Vartuli, J.C., Roth, W.J., Leonowicz, M.E., Kresge, C.T., Schmitt, K.D., Chu, C.T.W., Olson, D.H., Sheppard, E.W., McCullen, S.B., Higgins, J.B., Schlenker, J.L., 1992. A new family of mesoporous molecular sieves prepared with liquid crystal templates. J. Am. Chem. Soc. 114, 10834–10843.

Betageri, G.V., Makarla, K.R., 1995. Enhancement of dissolution of glyburide by solid dispersion and lyophilization techniques. Int. J. Pharm. 126, 155-160.

Beten, D.B., Amighi, K., Moës, A.J., 1995. Preparation of controlled-release coevaporates of dipyridamole by loading neutral pellets in a fluidized-bed coating system. Pharm. Res. 12, 1269-1272.

Bimbo, L.M., Sarparanta, M., Santos, H.A., Airaksinen, A.J., Mäkilä, E., Laaksonen, T., Peltonen, L., Lehto, V.-P., Hirvonen, J., Salonen, J., 2010. Biocompatibility of thermally hydrocarbonized porous silicon nanoparticles and their biodistribution in rats. ACS Nano 4, 3023-3032.

Bimbo, L.M., Mäkilä, E., Laaksonen, T., Lehto, V.-P., Salonen, J., Hirvonen, J., Santos, H.A., 2011. Drug permeation across intestinal epithelial cells using porous silicon nanoparticles. Biomaterials 32, 2625-2633.

Blagden, N., de Matas, M., Gavan, P.T., York, P., 2007. Crystal engineering of active pharmaceutical ingredients to improve solubility and dissolution rates. Adv. Drug Delivery Rev. 59, 617-630.

Blumen, S.R., Cheng, K., Ramos-Nino, M.E., Taatjes, D.J., Weiss, D.J., Landry, C.C., Mossman, B.T., 2007. Unique uptake of acid-prepared mesoporous spheres by lung epithelial and mesothelioma cells. Am. J. Respir. Cell Mol. Biol. 36, 333-342.

Boissière, C., Larbot, A., van der Lee, A., Kooyman, P.J., Prouzet, E., 2000. A new synthesis of mesoporous MSU-X silica controlled by a two-step pathway. Chem. Mater. 12, 2902-2913.

Borm, P.J.A., Schins, R.P.F., Albrecht, C., 2004. Inhaled particles and lung cancer, part B: Paradigms and risk assessment. Int. J. Cancer 110, 3-14.

Boukherroub, R., Petit, A., Loupy, A., Chazalviel, J.-N., Ozanam, F., 2003. Microwave-assisted chemical functionalization of hydrogen-terminated porous silicon surfaces. J. Phys. Chem. B 107, 13459-13462.

Bowditch, A.P., Waters, K., Gale, H., Rice, P., Scott, E.A.M., Canham, L.T., Reeves, C.L., Loni, A., Cox, T.I., 1999. In-vivo assessment of tissue compatibility and calcification of bulk and porous

silicon. In: Materials Research Society Symposium Proceedings 596. Materials Research Society, Warrendale, PA, USA, pp. 149-154.

Breitenbach, J., 2002. Melt extrusion: From process to drug delivery technology. Eur. J. Pharm. Biopharm. 54, 107-117.

Breitenbach, J., 2006. Melt extrusion can bring new benefits to HIV therapy. Am. J. Drug Deliv. 4, 61-64.

Brinker, C.J., Scherer, G.W., 1990. Sol-gel science: The physics and chemistry of sol-gel processing. Academic Press Inc, San Diego, CA, USA.

Buriak, J.M., Allen, M.J., 1998. Lewis acid mediated functionalization of porous silicon with substituted alkenes and alkynes. J. Am. Chem. Soc. 120, 1339-1340.

Burrows, V.A., Chabal, Y.J., Higashi, G.S., Raghavachari, K., Christman, S.B., 1988. Infrared spectroscopy of Si(111) surfaces after HF treatment: Hydrogen termination and surface morphology. Appl. Phys. Lett. 53, 998.

Bülau, H.C., Ulrich, J., 1997. Parameters influencing the properties of drop formed pastilles. In: CGOM4. Verlag Shaker, Aachen, Germany, pp. 123-130.

Cal, K., Sollohub, K., 2010. Spray drying technique. I: Hardware and process parameters. J. Pharm. Sci. 99, 575-586.

Calvert, G., Rice, F., Boiano, J., Sheehy, J., Sanderson, W., 2003. Occupational silica exposure and risk of various diseases: An analysis using death certificates from 27 states of the United States. Occup. Environ. Med. 60, 122-129.

Canham, L.T., 1990. Silicon quantum wire array fabrication by electrochemical and chemical dissolution of wafers. Appl. Phys. Lett. 57, 1046.

Canham, L.T., Houlton, M.R., Leong, W.Y., Pickering, C., Keen, J.M., 1991. Atmospheric impregnation of porous silicon at room temperature. J. Appl. Phys. 70, 422.

Canham, L.T., Reeves, C.L., 1995. Apatite nucleation on low porosity silicon in acellular simulated body fluids (abstract). MRS Online Proceedings Library 414, 189. doi: 10.1557/PROC-414-189.

Cauda, V., Mühlstein, L., Onida, B., Bein, T., 2009. Tuning drug uptake and release rates through different morphologies and pore diameters of confined mesoporous silica. Microporous Mesoporous Mater. 118, 435-442.

Cauda, V., Onida, B., Platschek, B., Mühlstein, L., Bein, T., 2008. Large antibiotic molecule diffusion in confined mesoporous silica with controlled morphology. J. Mater. Chem. 18, 5888-5899.

CDER/FDA, 2000. U.S. Food and Drug Administration, Center for Drug Evaluation and Research: Guidance for industry: Waiver of in vivo bioavailability and bioequivalence studies for immediate-release solid oral dosage forms based on a biopharmaceutics classification system. Retrieved February 23rd, 2011 from
http://www.fda.gov/downloads/Drugs/GuidanceComplianceRegulatoryInformation/Guidances/ucm070246.pdf

Chang, J.-S., Chang, K.L.B., Hwang, D.-F., Kong, Z.-L., 2007. In vitro cytotoxicitiy of silica nanoparticles at high concentrations strongly depends on the metabolic activity type of the cell line. Environ. Sci. Technol. 41, 2064-2068.

Charnay, C., Bégu, S., Tourné-Péteilh, C., Nicole, L., Lerner, D.A., Devoisselle, J.M., 2004. Inclusion of ibuprofen in mesoporous templated silica: Drug loading and release property. Eur. J. Pharm. Biopharm. 57, 533–540.

Chen, M., von Mikecz, A., 2005. Formation of nucleoplasmic protein aggregates impairs nuclear function in response to SiO_2 nanoparticles. Exp. Cell Res. 305, 51-62.

Chen, X., Vaughn, J.M., Yacaman, M.J., Williams, R.O., Johnston, K.P., 2004. Rapid dissolution of high-potency danazol particles produced by evaporative precipitation into aqueous solution. J. Pharm. Sci. 93, 1867-1878.

Chiappini, C., Tasciotti, E., Serda, R.E., Brousseau, L., Liu, X., Ferrari, M., 2011. Mesoporous silicon particles as intravascular drug delivery vectors: Fabrication, in-vitro, and in-vivo assessments. Phys. Status Solidi C 8, n/a. doi: 10.1002/pssc.201000344.

Chiou, W.L., Riegelman, S., 1971. Pharmaceutical applications of solid dispersion systems. J. Pharm. Sci. 60, 1281-1302.

Choi, J., Zhang, Q., Reipa, V., Wang, N.S., Stratmeyer, M.E., Hitchins, V.M., Goering, P.L., 2009. Comparison of cytotoxic and inflammatory responses of photoluminescent silicon nanoparticles with silicon micron-sized particles in RAW 264.7 macrophages. J Appl. Toxicol. 29, 52-60.

Chung, T.-H., Wu, S.-H., Yao, M., Lu, C.-W., Lin, Y.-S., Hung, Y., Mou, C.-Y., Chen, Y.-C., Huang, D.-M., 2007. The effect of surface charge on the uptake and biological function of mesoporous silica nanoparticles in 3T3-L1 cells and human mesenchymal stem cells. Biomaterials 28, 2959-2966.

Contessotto, L., Ghedini, E., Pinna, F., Signoretto, M., Cerrato, G., Crocellà, V., 2009. Hybrid organic-inorganic silica gel carriers with controlled drug-delivery properties. Chem. Eur. J. 15, 12043-12049.

Crowley, M.M., Zhang, F., Repka, M.A., Thumma, S., Upadhye, S.B., Battu, S.K., McGinity, J.W., Martin, C., 2007. Pharmaceutical applications of hot-melt extrusion: Part I. Drug Dev. Ind. Pharm. 33, 909-926.

Dahan, A., Miller, J.M., Amidon, G.L., 2009. Prediction of solubility and permeability class membership: Provisional BCS classification of the world's top oral drugs. AAPS J. 11, 740-746.

DeSesso, J.M., Jacobson, C.F., 2001. Anatomical and physiological parameters affecting gastrointestinal absorption in humans and rats. Food Chem. Toxicol. 39, 209-228.

Doadrio, J.C., Sousa, E.M.B., Izquierdo-Barba, I., Doadrio, A.L., Perez-Pariente, J., Vallet-Regí, M., 2006. Functionalization of mesoporous materials with long alkyl chains as a strategy for controlling drug delivery pattern. J. Mater. Chem. 16, 462-466.

Doshi, J., Reneker, D.H., 1995. Electrospinning process and applications of electrospun fibers. J. Electrostat. 35, 151-160.

van Drooge, D.-J., Hinrichs, W.L.J., Dickhoff, B.H.J., Elli, M.N.A., Visser, M.R., Zijlstra, G.S., Frijlink, H.W., 2005. Spray freeze drying to produce a stable Δ^9-tetrahydrocannabinol containing inulin-based solid dispersion powder suitable for inhalation. Eur. J. Pharm. Sci. 26, 231-240.

EMEA, 2010. European Medicines Agency, Committee for Medicinal Products for Human Use (CHMP): Guideline on the investigation of bioequivalence. Retrieved February 23rd, 2011 from http://www.ema.europa.eu/docs/en_GB/document_library/Scientific_guideline/2010/01/WC500070039.pdf

Euliss, L.E., DuPont, J.A., Gratton, S., DeSimone, J., 2006. Imparting size, shape, and composition control of materials for nanomedicine. Chem. Soc. Rev. 35, 1095-1104.

Fahr, A., Liu, X., 2007. Drug delivery strategies for poorly water-soluble drugs. Expert Opin. Drug Deliv. 4, 403-416.

Fathauer, R.W., George, T., Ksendzov, A., Vasquez, R.P., 1992. Visible luminescence from silicon wafers subjected to stain etches. Appl. Phys. Lett. 60, 995-997.

FDA, 1979. Database of Select Committee on GRAS Substances (SCOGS) Reviews: Silicon dioxides. Retrieved April 6th, 2011 from http://www.accessdata.fda.gov/scripts/fcn/fcnDetailNavigation.cfm?rpt=scogsListing&id=276.

FDA, 2011. Inactive ingredient search for approved drug products: Silicon dioxide. Retrieved April 6th, 2011 from http://www.accessdata.fda.gov/scripts/cder/iig.

Fenoglio, I., Croce, A., Di Renzo, F., Tiozzo, R., Fubini, B., 2000. Pure-silica zeolites (porosils) as model solids for the evaluation of the physicochemical features determining silica toxicity to macrophages. Chem. Res. Toxicol. 13, 489-500.

Foraker, A.B., Walczak, R.J., Cohen, M.H., Boiarski, T.A., Grove, C.F., Swaan, P.W., 2003. Microfabricated porous silicon particles enhance paracellular delivery of insulin across intestinal Caco-2 cell monolayers. Pharm. Res. 20, 110-116.

Francois, D., Jones, B.E., 1978. The hard capsule with the soft center. Paper presented at European Capsule Technology Symposium, pp 55-61. Information retrieved from Karanth et al., 2006.

Fu, Q., Rama Rao, G.V., Ward, T.L., Lu, Y., Lopez, G.P., 2007. Thermoresponsive transport through ordered mesoporous silica/PNIPAAm copolymer membranes and microspheres. Langmuir 23, 170-174.

Gilis, P.M.V., De Condé, V.F.V., Vandecruys, R.P.G., 1997. Beads having a core coated with an antifungal and a polymer, US Patent No. 5,633,015.

Giri, S., Trewyn, B.G., Stellmaker, M.P., Lin, V.S.-Y., 2005. Stimuli-responsive controlled-release delivery system based on mesoporous silica nanorods capped with magnetic nanoparticles. Angew. Chem. Int. Ed. 44, 5038-5044.

Goh, A.S.-W., Chung, A.Y.-F., Lo, R.H.-G., Lau, T.-N., Yu, S.W.-K., Chng, M., Satchithanantham, S., Loong, S.L.-E., Ng, D.C.-E., Lim, B.-C., Connor, S., Chow, P.K.-H., 2007. A novel approach to brachytherapy in hepatocellular carcinoma using a phosphorous^{32} (^{32}P) brachytherapy delivery device - a first-in-man study. Int. J. Radiation Oncology Biol. Phys. 67, 786-792.

Gomez-Orellana, I., 2005. Strategies to improve oral drug bioavailability. Expert Opin. Drug Deliv. 2, 419-433.

Gong, K., Viboonkiat, R., Rehman, I.U., Buckton, G., Darr, J.A., 2005. Formation and characterization of porous indomethacin-PVP coprecipitates prepared using solvent-free supercritical fluid processing. J. Pharm. Sci. 94, 2583-2590.

Greco, K., Bogner, R., 2010. Crystallization of amorphous indomethacin during dissolution: Effect of processing and annealing. Mol. Pharmaceutics 7, 1406-1418.

Gupta, M.K., Goldman, D., Bogner, R.H., Tseng, Y.-C., 2001. Enhanced drug dissolution and bulk properties of solid dispersions granulated with a surface adsorbent. Pharm. Dev. Technol. 6, 563-572.

Halimaoui, A., Oules, C., Bomchil, G., Bsiesy, A., Gaspard, F., Herino, R., Ligeon, M., Muller, F., 1991. Electroluminescence in the visible range during anodic oxidation of porous silicon films. Appl. Phys. Lett. 59, 304.

Han, Y.-J., Stucky, G.D., Butler, A., 1999. Mesoporous silicate sequestration and release of proteins. J. Am. Chem. Soc. 121, 9897-9898.

Hancock, B.C., Parks, M., 2000. What is the true solubility advantage for amorphous pharmaceuticals? Pharm. Res. 17, 397-404.

He, Q., Zhang, J., Chen, F., Guo, L., Zhu, Z., Shi, J., 2010. An anti-ROS/hepatic fibrosis drug delivery system based on salvianolic acid B loaded mesoporous silica nanoparticles. Biomaterials 31, 7785-7796.

He, Q., Zhang, Z., Gao, Y., Shi, J., Li, Y., 2009. Intracellular localization and cytotoxicity of spherical mesoporous silica nano- and microparticles. Small 5, 2722-2729.

He, X., Pei, L., Tong, H.H.Y., Zheng, Y., 2011. Comparison of spray freeze drying and the solvent evaporation method for preparing solid dispersions of baicalein with Pluronic F68 to improve dissolution and oral bioavailability. AAPS PharmSciTech, 12, 104-113.

Heikkilä, T., Salonen, J., Tuura, J., Hamdy, M.S., Mul, G., Kumar, N., Salmi, T., Murzin, D.Y., Laitinen, L., Kaukonen, A.M., Hirvonen, J., Lehto, V.-P., 2007a. Mesoporous silica material TUD-1 as a drug delivery system. Int. J. Pharm. 331, 133–138.

Heikkilä, T., Salonen, J., Tuura, J., Kumar, N., Salmi, T., Murzin, D.Y., Hamdy, M.S., Mul, G., Laitinen, L., Kaukonen, A.M., Hirvonen, J., Lehto, V.-P., 2007b. Evaluation of mesoporous TCPSi, MCM-41, SBA-15, and TUD-1 materials as API carriers for oral drug delivery. Drug Delivery 14, 337-347.

Heikkilä, T., Santos, H.A., Kumar, N., Murzin, D.Y., Salonen, J., Laaksonen, T., Peltonen, L., Hirvonen, J., Lehto, V.P., 2010. Cytotoxicity study of ordered mesoporous silica MCM-41 and SBA-15 microparticles on Caco-2 cells. Eur. J. Pharm. Biopharm. 74, 483-494.

Hench, L., West, J., 1990. The sol-gel process. Chem. Rev. 90, 33-72.

Hilgers, A.R., Conradi, R.A., Burton, P.S., 1990. Caco-2 cell monolayers as a model for drug transport across the intestinal mucosa. Pharm. Res. 7, 902-910.

Hillegass, J.M., Blumen, S.R., Cheng, K., MacPherson, M.B., Alexeeva, V., Lathrop, S.A., Beuschel, S.L., Steinbacher, J.L., Butnor, K.J., Ramos-Niño, M.E., Shukla, A., James, T.A., Weiss, D.J., Taatjes, D.J., Pass, H.I., Carbone, M., Landry, C.C., Mossman, B.T., 2011. Increased efficacy of doxorubicin delivered in multifunctional microparticles for mesothelioma therapy. Int. J. Cancer 129, 233-244.

Ho, H.-O., Su, H.-L., Tsai, T., Sheu, M.-T., 1996. The preparation and characterization of solid dispersions on pellets using a fluidized-bed system. Int. J. Pharm. 139, 223-229.

Holm, P., Buur, A., Elema, M., Onne, Mollgaard, B., Holm, J., Egeskov, Schultz, K., 2007. Controlled agglomeration, US Patent No. 7,217,431.

Horcajada, P., Rámila, A., Férey, G., Vallet-Regí, M., 2006. Influence of superficial organic modification of MCM-41 matrices on drug delivery rate. Solid State Sci. 8, 1243-1249.

Horcajada, P., Rámila, A., Pérez-Pariente, J., Vallet-Regı, M., 2004. Influence of pore size of MCM-41 matrices on drug delivery rate. Microporous and Mesoporous Materials 68, 105–109.

Hsiao, J.-K., Tsai, C.-P., Chung, T.-H., Hung, Y., Yao, M., Liu, H.-M., Mou, C.-Y., Yang, C.-S., Chen, Y.-C., Huang, D.-M., 2008. Mesoporous silica nanoparticles as a delivery system of gadolinium for effective human stem cell tracking. Small 4, 1445-1452.

Huang, L.-F., Tong, W.-Q., 2004. Impact of solid state properties on developability assessment of drug candidates. Adv. Drug Delivery Rev. 56, 321-334.

Huang, S., Fan, Y., Cheng, Z., Kong, D., Yang, P., Quan, Z., Zhang, C., Lin, J., 2009. Magnetic mesoporous silica spheres for drug targeting and controlled release. J. Phys. Chem. C 113, 1775-1784.

Huang, X., El-Sayed, I.H., Qian, W., El-Sayed, M.A., 2006. Cancer cell imaging and photothermal therapy in the near-infrared region by using gold nanorods. J. Am. Chem. Soc. 128, 2115-2120.

Huang, X., Teng, X., Chen, D., Tang, F., He, J., 2010. The effect of the shape of mesoporous silica nanoparticles on cellular uptake and cell function. Biomaterials 31, 438-448.

Hubatsch, I., Ragnarsson, E.G.E., Artursson, P., 2007. Determination of drug permeability and prediction of drug absorption in Caco-2 monolayers. Nat. Protocols 2, 2111-2119.

Hudson, S.P., Padera, R.F., Langer, R., Kohane, D.S., 2008. The biocompatibility of mesoporous silicates. Biomaterials 29, 4045-4055.

Huh, S., Chen, H.-T., Wiench, J.W., Pruski, M., Lin, V.S.-Y., 2005. Cooperative catalysis by general acid and base bifunctionalized mesoporous silica nanospheres. Angew. Chem. Int. Ed. 44, 1826-1830.

Hämäläinen, M.D., Frostell-Karlsson, A., 2004. Predicting the intestinal absorption potential of hits and leads. Drug Discov. Today Technol. 1, 397-405.

Hörter, D., Dressman, J.B., 1997. Influence of physicochemical properties on dissolution of drugs in the gastrointestinal tract. Adv. Drug Delivery Rev. 25, 3-14.

IARC, 1997. IARC working group on the evaluation of carcinogenic risks to humans. Silica, some silicates, coal dust and para-aramid fibrils. World Health Organization, IARCPress, UK.

Iler, R.K., 1979. Chemistry of silica - solubility, polymerization, colloid and surface properties and biochemistry. John Wiley & Sons, New York, USA.

Izquierdo-Barba, I., Martinez, Á., Doadrio, A.L., Pérez-Pariente, J., Vallet-Regí, M., 2005. Release evaluation of drugs from ordered three-dimensional silica structures. Eur. J. Pharm. Sci. 26, 365-373.

Jakubowicz, J., Smardz, K., Smardz, L., 2007. Characterization of porous silicon prepared by powder technology. Physica E Low Dimens. Syst. Nanostruct. 38, 139-143.

Jannin, V., Musakhanian, J., Marchaud, D., 2008. Approaches for the development of solid and semi-solid lipid-based formulations. Adv. Drug Delivery Rev. 60, 734-746.

Janssens, S., Van den Mooter, G., 2009. Review: Physical chemistry of solid dispersions. J. Pharm. Pharmacol. 61, 1571-1586.

Jugdaohsingh, R., Anderson, S.H., Tucker, K.L., Elliott, H., Kiel, D.P., Thompson, R.P., Powell, J.J., 2002. Dietary silicon intake and absorption. Am. J. Clin. Nutr. 75, 887 -893.

Jugdaohsingh, R., Tucker, K.L., Qiao, N., Cupples, L.A., Kiel, D.P., Powell, J.J., 2003. Dietary silicon intake is positively associated with bone mineral density in men and premenopausal women of the Framingham Offspring cohort. J. Bone Miner. Res. 19, 297-307.

Kansy, M., Senner, F., Gubernator, K., 1998. Physicochemical high throughput screening: Parallel artificial membrane permeation assay in the description of passive absorption processes. J. Med. Chem. 41, 1007-1010.

Karanth, H., Shenoy, V.S., Murthy, R.R., 2006. Industrially feasible alternative approaches in the manufacture of solid dispersions: A technical report. AAPS PharmSciTech 7, E31-E38.

Kawakami, K., 2009. Current status of amorphous formulation and other special dosage forms as formulations for early clinical phases. J. Pharm. Sci. 98, 2875-2885.

Kenawy, E.-R., Bowlin, G.L., Mansfield, K., Layman, J., Simpson, D.G., Sanders, E.H., Wnek, G.E., 2002. Release of tetracycline hydrochloride from electrospun poly(ethylene-co-vinylacetate), poly(lactic acid), and a blend. J. Controlled Release 81, 57-64.

Kerns, E.H., Di, L., 2003. Pharmaceutical profiling in drug discovery. Drug Discov. Today 8, 316-323.

Kilpeläinen, M., Mönkäre, J., Vlasova, M.A., Riikonen, J., Lehto, V.-P., Salonen, J., Järvinen, K., Herzig, K.-H., 2011. Nanostructured porous silicon microparticles enable sustained peptide (Melanotan II) delivery. Eur. J. Pharm. Biopharm. 77, 20-25.

Kilpeläinen, M., Riikonen, J., Vlasova, M.A., Huotari, A., Lehto, V.P., Salonen, J., Herzig, K.H., Järvinen, K., 2009. In vivo delivery of a peptide, ghrelin antagonist, with mesoporous silicon microparticles. J. Controlled Release 137, 166-170.

Kim, H.-J., Matsuda, H., Zhou, H., Honma, I., 2006. Ultrasound-triggered smart drug release from a poly(dimethylsiloxane)–mesoporous silica composite. Adv. Mater. 18, 3083-3088.

Kim, J., Kim, H.S., Lee, N., Kim, T., Kim, H., Yu, T., Song, I.C., Moon, W.K., Hyeon, T., 2008. Multifunctional uniform nanoparticles composed of a magnetite nanocrystal core and a

mesoporous silica shell for magnetic resonance and fluorescence imaging and for drug delivery. Angew. Chem. 120, 8566-8569.

Kinnari, P., Mäkilä, E., Heikkilä, T., Salonen, J., Hirvonen, J., Santos, H.A., 2011. Comparison of mesoporous silicon and non-ordered mesoporous silica materials as drug carriers for itraconazole. Int. J. Pharm. n/a, n/a. doi:10.1016/j.ijpharm.2011.05.021.

Kortesuo, P., Ahola, M., Karlsson, S., Kangasniemi, I., Yli-Urpo, A., Kiesvaara, J., 2000. Silica xerogel as an implantable carrier for controlled drug delivery - evaluation of drug distribution and tissue effects after implantation. Biomaterials 21, 193-198.

Kosuge, K., Sato, T., Kikukawa, N., Takemori, M., 2004. Morphological control of rod- and fiberlike SBA-15 type mesoporous silica using water-soluble sodium silicate. Chem. Mater. 16, 899-905.

Kozlova, S.A., Kirik, S.D., 2010. Post-synthetic activation of silanol covering in the mesostructured silicate materials MSM-41 and SBA-15. Microporous Mesoporous Mater. 133, 124-133.

Kresge, C.T., Leonowicz, M.E., Roth, W.J., Vartuli, J.C., Beck, J.S., 1992. Ordered mesoporous molecular sieves synthesized by a liquid-crystal template mechanism. Nature 359, 710-712.

Lai, C.-Y., Trewyn, B.G., Jeftinija, D.M., Jeftinija, K., Xu, S., Jeftinija, S., Lin, V.S.-Y., 2003. A mesoporous silica nanosphere-based carrier system with chemically removable CdS nanoparticle caps for stimuli-responsive controlled release of neurotransmitters and drug molecules. J. Am. Chem. Soc. 125, 4451-4459.

Lakshman, J.P., Cao, Y., Kowalski, J., Serajuddin, A.T.M., 2008. Application of melt extrusion in the development of a physically and chemically stable high-energy amorphous solid dispersion of a poorly water-soluble drug. Mol. Pharmaceutics 5, 994-1002.

Laza-Knoerr, A.L., Gref, R., Couvreur, P., 2010. Cyclodextrins for drug delivery. J. Drug Targeting 18, 645-656.

Lee, C.-H., Cheng, S.-H., Wang, Y.-J., Chen, Y.-C., Chen, N.-T., Souris, J., Chen, C.-T., Mou, C.-Y., Yang, C.-S., Lo, L.-W., 2009. Near-infrared mesoporous silica nanoparticles for optical imaging: Characterization and in vivo biodistribution. Adv. Funct. Mater. 19, 215-222.

Lee, C.-H., Lo, L.-W., Mou, C.-Y., Yang, C.-S., 2008. Synthesis and characterization of positive-charge functionalized mesoporous silica nanoparticles for oral drug delivery of an anti-inflammatory drug. Adv. Funct. Mater. 18, 3283-3292.

Lehmann, V., Grüning, U., 1997. The limits of macropore array fabrication. Thin Solid Films 297, 13-17.

Lehmann, V., Stengl, R., Luigart, A., 2000. On the morphology and the electrochemical formation mechanism of mesoporous silicon. Mater. Sci. Eng., B 69-70, 11-22.

Lennernäs, H., Abrahamsson, B., 2005. The use of biopharmaceutic classification of drugs in drug discovery and development: Current status and future extension. J. Pharm. Pharmacol. 57, 273-285.

Leuner, C., Dressman, J., 2000. Improving drug solubility for oral delivery using solid dispersions. Eur. J. Pharm. Biopharm. 50, 47-60.

Li, J., Guo, Y., Zografi, G., 2002. The solid-state stability of amorphous quinapril in the presence of β-cyclodextrins. J. Pharm. Sci. 91, 229-243.

Lin, W., Huang, Y.-wern, Zhou, X.-D., Ma, Y., 2006. In vitro toxicity of silica nanoparticles in human lung cancer cells. Toxicol. Appl. Pharmacol. 217, 252-259.

Lin, V.S.-Y., Motesharei, K., Dancil, K.-P.S., Sailor, M.J., Ghadiri, M.R., 1997. A porous silicon-based optical interferometric biosensor. Science 278, 840 -843.

Lin, Y.-S., Haynes, C.L., 2010. Impacts of mesoporous silica nanoparticle size, pore ordering, and pore integrity on hemolytic activity. J. Am. Chem. Soc. 132, 4834-4842.

Lin, Y.-S., Tsai, C.-P., Huang, H.-Y., Kuo, C.-T., Hung, Y., Huang, D.-M., Chen, Y.-C., Mou, C.-Y., 2005. Well-ordered mesoporous silica nanoparticles as cell markers. Chem. Mater. 17, 4570-4573.

Linford, M.R., Chidsey, C.E.D., 1993. Alkyl monolayers covalently bonded to silicon surfaces. J. Am. Chem. Soc. 115, 12631-12632.

Liu, H.-M., Wu, S.-H., Lu, C.-W., Yao, M., Hsiao, J.-K., Hung, Y., Lin, Y.-S., Mou, C.-Y., Yang, C.-S., Huang, D.-M., Chen, Y.-C., 2008. Mesoporous silica nanoparticles improve magnetic labeling efficiency in human stem cells. Small 4, 619-626.

Liu, X., Sun, J., 2010. Endothelial cells dysfunction induced by silica nanoparticles through oxidative stress via JNK/P53 and NF-κB pathways. Biomaterials 31, 8198-8209.

López, T., Basaldella, E.I., Ojeda, M.L., Manjarrez, J., Alexander-Katz, R., 2006. Encapsulation of valproic acid and sodic phenytoin in ordered mesoporous SiO_2 solids for the treatment of temporal lobe epilepsy. Opt. Mater. 29, 75-81.

Low, S.P., Voelcker, N.H., Canham, L.T., Williams, K.A., 2009. The biocompatibility of porous silicon in tissues of the eye. Biomaterials 30, 2873-2880.

Lu, J., Liong, M., Li, Z., Zink, J.I., Tamanoi, F., 2010. Biocompatibility, biodistribution, and drug-delivery efficiency of mesoporous silica nanoparticles for cancer therapy in animals. Small 6, 1794-1805.

Mal, N.K., Fujiwara, M., Tanaka, Y., 2003. Photocontrolled reversible release of guest molecules from coumarin-modified mesoporous silica. Nature 421, 350-353.

Manzano, M., Aina, V., Areán, C.O., Balas, F., Cauda, V., Colilla, M., Delgado, M.R., Vallet-Regí, M., 2008. Studies on MCM-41 mesoporous silica for drug delivery: Effect of particle morphology and amine functionalization. Chem. Eng. J. 137, 30-37.

Mattei, G., Alieva, E.V., Petrov, J.E., Yakovlev, V.A., 2000. Quick oxidation of porous silicon in presence of pyridine vapor. Phys. Status Solidi A 182, 139-143.

Mellaerts, R., Aerts, C.A., Humbeeck, J.V., Augustijns, P., den Mooter, G.V., Martens, J.A., 2007. Enhanced release of itraconazole from ordered mesoporous SBA-15 silica materials. Chem. Commun. n/a, 1375-1377.

Mellaerts, R., Jammaer, J.A.G., Van Speybroeck, M., Chen, H., Humbeeck, J.V., Augustijns, P., Van den Mooter, G., Martens, J.A., 2008a. Physical state of poorly water soluble therapeutic molecules loaded into SBA-15 ordered mesoporous silica carriers: A case study with itraconazole and ibuprofen. Langmuir 24, 8651-8659.

Mellaerts, R., Mols, R., Jammaer, J.A.G., Aerts, C.A., Annaert, P., Van Humbeeck, J., Van den Mooter, G., Augustijns, P., Martens, J.A., 2008b. Increasing the oral bioavailability of the poorly water soluble drug itraconazole with ordered mesoporous silica. Eur. J. Pharm. Biopharm. 69, 223-230.

Merget, R., Bauer, T., Küpper, H., Philippou, S., Bauer, H., Breitstadt, R., Bruening, T., 2002. Health hazards due to the inhalation of amorphous silica. Arch. Toxicol. 75, 625-634.

Miura, H., Kanebako, M., Shirai, H., Nakao, H., Inagi, T., Terada, K., 2010. Enhancement of dissolution rate and oral absorption of a poorly water-soluble drug, K-832, by adsorption onto porous silica using supercritical carbon dioxide. Eur. J. Pharm. Biopharm. 76, 215-221.

Miura, H., Kanebako, M., Shirai, H., Nakao, H., Inagi, T., Terada, K., 2011. Stability of amorphous drug, 2-benzyl-5-(4-chlorophenyl)-6-[4-(methylthio)phenyl]-2H-pyridazin-3-one, in silica mesopores and measurement of its molecular mobility by solid-state ^{13}C NMR spectroscopy. Int. J. Pharm. 410, 61-67.

Moghimi, S.M., Szebeni, J., 2003. Stealth liposomes and long circulating nanoparticles: Critical issues in pharmacokinetics, opsonization and protein-binding properties. Prog. Lipid Res. 42, 463-478.

Muñoz, B., Rámila, A., Pérez-Pariente, J., Díaz, I., Vallet-Regí, M., 2003. MCM-41 organic modification as drug delivery rate regulator. Chem. Mater. 15, 500-503.

Nandiyanto, A.B.D., Kim, S.-G., Iskandar, F., Okuyama, K., 2009. Synthesis of spherical mesoporous silica nanoparticles with nanometer-size controllable pores and outer diameters. Microporous Mesoporous Mater. 120, 447-453.

Nieto, A., Balas, F., Colilla, M., Manzano, M., Vallet-Regí, M., 2008. Functionalization degree of SBA-15 as key factor to modulate sodium alendronate dosage. Microporous Mesoporous Mater. 116, 4-13.

Noguchi, N., Suemune, I., 1993. Luminescent porous silicon synthesized by visible light irradiation. Appl. Phys. Lett. 62, 1429-1431.

Ohta, K.M., Fuji, M., Takei, T., Chikazawa, M., 2005. Development of a simple method for the preparation of a silica gel based controlled delivery system with a high drug content. Eur. J. Pharm. Sci. 26, 87-96.

Park, J.-H., Gu, L., von Maltzahn, G., Ruoslahti, E., Bhatia, S.N., Sailor, M.J., 2009. Biodegradable luminescent porous silicon nanoparticles for in vivo applications. Nat. Mater. 8, 331-336.

Park, E.-J., Park, K., 2009. Oxidative stress and pro-inflammatory responses induced by silica nanoparticles in vivo and in vitro. Toxicol. Lett. 184, 18-25.

Di Pasqua, A.J., Sharma, K.K., Shi, Y.-L., Toms, B.B., Ouellette, W., Dabrowiak, J.C., Asefa, T., 2008. Cytotoxicity of mesoporous silica nanomaterials. J. Inorg. Biochem. 102, 1416-1423.

Passerini, N., Albertini, B., González-Rodríguez, M.L., Cavallari, C., Rodriguez, L., 2002. Preparation and characterisation of ibuprofen-poloxamer 188 granules obtained by melt granulation. Eur. J. Pharm. Sci. 15, 71-78.

Passerini, N., Albertini, B., Perissutti, B., Rodriguez, L., 2006. Evaluation of melt granulation and ultrasonic spray congealing as techniques to enhance the dissolution of praziquantel. Int. J. Pharm. 318, 92-102.

Passerini, N., Calogerà, G., Albertini, B., Rodriguez, L., 2010. Melt granulation of pharmaceutical powders: A comparison of high-shear mixer and fluidised bed processes. Int. J. Pharm. 391, 177-186.

Patel, R.P., Suthar, A., 2009. Formulation and process optimization of cinnarizine fast-release tablets. Pharm. Tech. 33, 53-59.

Perissutti, B., Rubessa, F., Moneghini, M., Voinovich, D., 2003. Formulation design of carbamazepine fast-release tablets prepared by melt granulation technique. Int. J. Pharm. 256, 53-63.

Petrova-Koch, V., Muschik, T., Kux, A., Meyer, B. K., Koch, F., Lehmann, V., 1992. Rapid-thermal-oxidized porous Si - the superior photoluminescent Si. Appl. Phys. Lett. 61, 943-945.

Planinsek, O., Kovacic, B., Vrecer, F., 2011. Carvedilol dissolution improvement by preparation of solid dispersions with porous silica. Int. J. Pharm. 406, 41-48.

Popovici, R.F., Seftel, E.M., Mihai, G.D., Popovici, E., Voicu, V.A., 2011. Controlled drug delivery system based on ordered mesoporous silica matrices of captopril as angiotensin-converting enzyme inhibitor drug. J. Pharm. Sci. 100, 704-714.

Porter, C.J.H., Pouton, C.W., Cuine, J.F., Charman, W.N., 2008. Enhancing intestinal drug solubilisation using lipid-based delivery systems. Adv. Drug Delivery Rev. 60, 673-691.

Pouton, C.W., 2000. Lipid formulations for oral administration of drugs: Non-emulsifying, self-emulsifying and 'self-microemulsifying' drug delivery systems. Eur. J. Pharm. Sci. 11, S93-S98.

pSivida Corp., 2011. pSivida Corporation Homepage and News Releases. Retrieved May 6th, 2011 from http://www.psivida.com.

Pudipeddi, M., Serajuddin, A.T.M., 2005. Trends in solubility of polymorphs. J. Pharm. Sci. 94, 929-939.

Qian, F., Huang, J., Hussain, M.A., 2010. Drug-polymer solubility and miscibility: Stability consideration and practical challenges in amorphous solid dispersion development. J. Pharm. Sci. 99, 2941-2947.

Qu, F., Zhu, G., Huang, S., Li, S., Sun, J., Zhang, D., Qiu, S., 2006a. Controlled release of captopril by regulating the pore size and morphology of ordered mesoporous silica. Microporous Mesoporous Mater. 92, 1–9.

Qu, F., Zhu, G., Lin, H., Zhang, W., Sun, J., Li, S., Qiu, S., 2006b. A controlled release of ibuprofen by systematically tailoring the morphology of mesoporous silica materials. J. Solid State Chem. 179, 2027-2035.

Radin, S., El-Bassyouni, G., Vresilovic, E.J., Schepers, E., Ducheyne, P., 2005. In vivo tissue response to resorbable silica xerogels as controlled-release materials. Biomaterials 26, 1043-1052.

Radu, D.R., Lai, C.-Y., Huang, J., Shu, X., Lin, V.S.-Y., 2005. Fine-tuning the degree of organic functionalization of mesoporous silica nanosphere materials via an interfacially designed co-condensation method. Chem. Commun. n/a, 1264-1266.

Reffitt, D.M., Jugdaohsingh, R., Thompson, R.P.H., Powell, J.J., 1999. Silicic acid: Its gastrointestinal uptake and urinary excretion in man and effects on aluminium excretion. J. Inorg. Biochem. 76, 141-147.

Repka, M.A., Battu, S.K., Upadhye, S.B., Thumma, S., Crowley, M.M., Zhang, F., Martin, C., McGinity, J.W., 2007. Pharmaceutical applications of hot-melt extrusion: Part II. Drug Dev. Ind. Pharm. 33, 1043-1057.

Reynhardt, J.P.K., Yang, Y., Sayari, A., Alper, H., 2005. Polyamidoamine dendrimers prepared inside the channels of pore-expanded periodic mesoporous silica. Adv. Funct. Mater. 15, 1641-1646.

Rigby, S.P., Fairhead, M., Van der Waller, C.F., 2008. Engineering silica particles as oral drug delivery vehicles. Curr. Pharm. Des. 14, 1821-1831.

Rodriguez, L., Passerini, N., Cavallari, C., Cini, M., Sancin, P., Fini, A., 1999. Description and preliminary evaluation of a new ultrasonic atomizer for spray-congealing processes. Int. J. Pharm. 183, 133-143.

Rosengren, A., Wallman, L., Bengtsson, M., Laurell, T., Danielsen, N., Bjursten, L.M., 2000. Tissue reactions to porous silicon: A comparative biomaterial study. Phys. Status Solidi A 182, 527-531.

Rouquerol, J., Avnir, D., Fairbridge, C.W., Everett, D.H., Haynes, J.M., Pernicone, N., Ramsay, J.D.F., Sing, K.S.W., Unger, K.K., 1994. Recommendations for the characterization of porous solids (technical report). Pure Appl. Chem. 66, 1739-1758.

Rowe, T.W.G., 1960. The theory and practice of freeze-drying. Ann. N. Y. Acad. Sci. 85, 641-681.

Salonen, J., Björkqvist, M., Laine, E., Niinistö, L., 2000a. Effects of fabrication parameters on porous p^+-type silicon morphology. Phys. Status Solidi A 182, 249-254.

Salonen, J., Björkqvist, M., Laine, E., Niinistö, L., 2004. Stabilization of porous silicon surface by thermal decomposition of acetylene. Appl. Surf. Sci. 225, 389-394.

Salonen, J., Kaukonen, A.M., Hirvonen, J., Lehto, V.-P., 2008. Mesoporous silicon in drug delivery applications. J. Pharm. Sci. 97, 632-653.

Salonen, J., Laitinen, L., Kaukonen, A.M., Tuura, J., Björkqvist, M., Heikkilä, T., Vähä-Heikkilä, K., Hirvonen, J., Lehto, V.P., 2005. Mesoporous silicon microparticles for oral drug delivery: Loading and release of five model drugs. J. Controlled Release 108, 362–374.

Salonen, J., Lehto, V.-P., 1997. Thermal oxidation of free-standing porous silicon films. Appl. Phys. Lett. 70, 637.

Salonen, J., Lehto, V.-P., 2008. Fabrication and chemical surface modification of mesoporous silicon for biomedical applications. Chem. Eng. J. 137, 162-172.

Salonen, J., Lehto, V.-P., Björkqvist, M., Laine, E., Niinistö, L., 2000b. Studies of thermally-carbonized porous silicon surfaces. Phys. Status Solidi A 182, 123-126.

Salonen, J., Lehto, V.-P., Laine, E., 1997. The room temperature oxidation of porous silicon. Appl. Surf. Sci. 120, 191-198.

Santos, H.A., Riikonen, J., Salonen, J., Mäkilä, E., Heikkilä, T., Laaksonen, T., Peltonen, L., Lehto, V.-P., Hirvonen, J., 2010. In vitro cytotoxicity of porous silicon microparticles: Effect of the particle concentration, surface chemistry and size. Acta Biomater. 6, 2721-2731.

Sarkari, M., Brown, J., Chen, X., Swinnea, S., Williams, R.O., Johnston, K.P., 2002. Enhanced drug dissolution using evaporative precipitation into aqueous solution. Int. J. Pharm. 243, 17-31.

Sekiguchi, K., Obi, N., 1961. Studies on absorption of eutectic mixture: I. A comparison of the behavior of eutectic mixture of sulfathiazole and that of ordinary sulfathiazole in man. Chem. Pharm. Bull. 9, 866-872.

Seo, A., Holm, P., Kristensen, H.G., Schæfer, T., 2003. The preparation of agglomerates containing solid dispersions of diazepam by melt agglomeration in a high shear mixer. Int. J. Pharm. 259, 161-171.

Serajuddin, A.T.M., 1999. Solid dispersion of poorly water-soluble drugs: Early promises, subsequent problems, and recent breakthroughs. J. Pharm. Sci. 88, 1058-1066.

Sethia, S., Squillante, E., 2002. Physicochemical characterization of solid dispersions of carbamazepine formulated by supercritical carbon dioxide and conventional solvent evaporation method. J. Pharm. Sci. 91, 1948-1957.

Shegokar, R., Müller, R.H., 2010. Nanocrystals: Industrially feasible multifunctional formulation technology for poorly soluble actives. Int. J. Pharm. 399, 129-139.

Shen, S.-C., Ng, W.K., Chia, L., Dong, Y.-C., Tan, R.B.H., 2009. Stabilized amorphous state of ibuprofen by co-spray drying with mesoporous SBA-15 to enhance dissolution properties. J. Pharm. Sci., 1997-2007.

Shen, S.-C., Ng, W.K., Chia, L., Hu, J., Tan, R.B.H., 2011. Physical state and dissolution of ibuprofen formulated by co-spray drying with mesoporous silica: Effect of pore and particle size. Int. J. Pharm. 410, 188-195.

Shenderovich, I.G., Buntkowsky, G., Schreiber, A., Gedat, E., Sharif, S., Albrecht, J., Golubev, N.S., Findenegg, G.H., Limbach, H.-H., 2003. Pyridine-^{15}N - a mobile NMR sensor for surface acidity and surface defects of mesoporous silica. J. Phys. Chem. B 107, 11924-11939.

Shih, S., Jung, K.H., Hsieh, T.Y., Sarathy, J., Campbell, J.C., Kwong, D.L., 1992. Photoluminescence and formation mechanism of chemically etched silicon. Appl. Phys. Lett. 60, 1863-1865.

Sinswat, P., Gao, X., Yacaman, M.J., Williams III, R.O., Johnston, K.P., 2005. Stabilizer choice for rapid dissolving high potency itraconazole particles formed by evaporative precipitation into aqueous solution. Int. J. Pharm. 302, 113-124.

Slowing, I., Trewyn, B.G., Lin, V.S.-Y., 2006. Effect of surface functionalization of MCM-41-type mesoporous silica nanoparticles on the endocytosis by human cancer cells. J. Am. Chem. Soc. 128, 14792-14793.

Slowing, I.I., Vivero-Escoto, J.L., Wu, C.-W., Lin, V.S.-Y., 2008. Mesoporous silica nanoparticles as controlled release drug delivery and gene transfection carriers. Adv. Drug Delivery Rev. 60, 1278-1288.

Smirnova, I., Mamic, J., Arlt, W., 2003. Adsorption of drugs on silica aerogels. Langmuir 19, 8521-8525.

Smirnova, I., Suttiruengwong, S., Seiler, M., Arlt, W., 2005. Dissolution rate enhancement by adsorption of poorly soluble drugs on hydrophilic silica aerogels. Pharm. Dev. Technol. 9, 443-452.

Sollohub, K., Cal, K., 2010. Spray drying technique: II. Current applications in pharmaceutical technology. J. Pharm. Sci. 99, 587-597.

Song, J.H., Sailor, M.J., 1998. Functionalization of nanocrystalline porous silicon Surfaces with aryllithium reagents: Formation of silicon−carbon bonds by cleavage of silicon−silicon bonds. J. Am. Chem. Soc. 120, 2376-2381.

Song, S.-W., Hidajat, K., Kawi, S., 2005. Functionalized SBA-15 materials as carriers for controlled drug delivery: Influence of surface properties on matrix−drug interactions. Langmuir 21, 9568-9575.

Van Speybroeck, M., Barillaro, V., Thi, T.D., Mellaerts, R., Martens, J., Van Humbeeck, J., Vermant, J., Annaert, P., Van den Mooter, G., Augustijns, P., 2009. Ordered mesoporous silica material SBA-15: A broad-spectrum formulation platform for poorly soluble drugs. J. Pharm. Sci. 98, 2648-2658.

Van Speybroeck, M., Mellaerts, R., Mols, R., Thi, T.D., Martens, J.A., Van Humbeeck, J., Annaert, P., Van den Mooter, G., Augustijns, P., 2010a. Enhanced absorption of the poorly soluble drug fenofibrate by tuning its release rate from ordered mesoporous silica. Eur. J. Pharm. Sci. 41, 623-630.

Van Speybroeck, M., Mols, R., Mellaerts, R., Thi, T.D., Martens, J.A., Humbeeck, J.V., Annaert, P., Mooter, G.V. den, Augustijns, P., 2010b. Combined use of ordered mesoporous silica and precipitation inhibitors for improved oral absorption of the poorly soluble weak base itraconazole. Eur. J. Pharm. Biopharm. 75, 354-365.

Sripanyakorn, S., Jugdaohsingh, R., Thompson, R.P.H., Powell, J.J., 2005. Dietary silicon and bone health. Nutr. Bulletin 30, 222-230.

Steinbacher, J.L., Lathrop, S.A., Cheng, K., Hillegass, J.M., Butnor, K.J., Kauppinen, R.A., Mossman, B.T., Landry, C.C., 2010. Gd-labeled microparticles in MRI: In vivo imaging of microparticles after intraperitoneal injection. Small 6, 2678-2682.

Stewart, M.P., Buriak, J.M., 2000. Chemical and biological applications of porous silicon technology. Adv. Mater. 12, 859-869.

Takeuchi, H., Nagira, S., Yamamoto, H., Kawashima, Y., 2004. Solid dispersion particles of tolbutamide prepared with fine silica particles by the spray-drying method. Powder Technol. 141, 187-195.

Takeuchi, H., Nagira, S., Yamamoto, H., Kawashima, Y., 2005. Solid dispersion particles of amorphous indomethacin with fine porous silica particles by using spray-drying method. Int. J. Pharm. 293, 155-164.

Tanaka, T., Godin, B., Bhavane, R., Nieves-Alicea, R., Gu, J., Liu, X., Chiappini, C., Fakhoury, J.R., Amra, S., Ewing, A., Li, Q., Fidler, I.J., Ferrari, M., 2010a. In vivo evaluation of safety of nanoporous silicon carriers following single and multiple dose intravenous administrations in mice. Int. J. Pharm. 402, 190-197.

Tanaka, T., Mangala, L.S., Vivas-Mejia, P.E., Nieves-Alicea, R., Mann, A.P., Mora, E., Han, H.-D., Shahzad, M.M.K., Liu, X., Bhavane, R., Gu, J., Fakhoury, J.R., Chiappini, C., Lu, C., Matsuo, K., Godin, B., Stone, R.L., Nick, A.M., Lopez-Berestein, G., Sood, A.K., Ferrari, M., 2010b. Sustained small interfering RNA delivery by mesoporous silicon particles. Cancer Res. 70, 3687 - 3696.

Tanev, P.T., Pinnavaia, T.J., 1995. A neutral templating route to mesoporous molecular sieves. Science 267, 865 -867.

Tang, X. (C.), Pikal, M.J., 2004. Design of freeze-drying processes for pharmaceuticals: Practical advice. Pharm. Res. 21, 191-200.

Tao, Z., Morrow, M.P., Asefa, T., Sharma, K.K., Duncan, C., Anan, A., Penefsky, H.S., Goodisman, J., Souid, A.-K., 2008. Mesoporous silica nanoparticles inhibit cellular respiration. Nano Lett. 8, 1517-1526.

Tasciotti, E., Liu, X., Bhavane, R., Plant, K., Leonard, A.D., Price, B.K., Cheng, M.M.-C., Decuzzi, P., Tour, J.M., Robertson, F., Ferrari, M., 2008. Mesoporous silicon particles as a multistage delivery system for imaging and therapeutic applications. Nat. Nano 3, 151-157.

Taylor, K.M.L., Kim, J.S., Rieter, W.J., An, H., Lin, W., Lin, W., 2008. Mesoporous silica nanospheres as highly efficient MRI contrast agents. J. Am. Chem. Soc. 130, 2154-2155.

Thies, R., Kleinebudde, P., 1999. Melt pelletisation of a hygroscopic drug in a high shear mixer: Part 1. Influence of process variables. Int. J. Pharm. 188, 131-143.

Thomas, M.J.K., Slipper, I., Walunj, A., Jain, A., Favretto, M.E., Kallinteri, P., Douroumis, D., 2010. Inclusion of poorly soluble drugs in highly ordered mesoporous silica nanoparticles. Int. J. Pharm. 387, 272-277.

Tomita, M., Hayashi, M., Awazu, S., 1996. Absorption-enhancing mechanism of EDTA, caprate, and decanoylcarnitine in Caco-2 cells. J. Pharm. Sci. 85, 608-611.

Tong, H.H.Y., Du, Z., Wang, G.N., Chan, H.M., Chang, Q., Lai, L.C.M., Chow, A.H.L., Zheng, Y., 2011. Spray freeze drying with polyvinylpyrrolidone and sodium caprate for improved dissolution and oral bioavailability of oleanolic acid, a BCS Class IV compound. Int. J. Pharm. 404, 148-158.

Vaccari, L., Canton, D., Zaffaroni, N., Villa, R., Tormen, M., di Fabrizio, E., 2006. Porous silicon as drug carrier for controlled delivery of doxorubicin anticancer agent. Microelectron. Eng. 83, 1598-1601.

Walker, G.M., Bell, S.E.J., Andrews, G., Jones, D., 2007. Co-melt fluidised bed granulation of pharmaceutical powders: Improvements in drug bioavailability. Chem. Eng. Sci. 62, 451-462.

Vallet-Regí, M., 2006. Ordered mesoporous materials in the context of drug delivery systems and bone tissue engineering. Chem. Eur. J. 12, 5934-5943.

Vallet-Regí, M., 2010. Nanostructured mesoporous silica matrices in nanomedicine. J. Intern. Med. 267, 22-43.

Vallet-Regí, M., Rámila, A., del Real, R.P., Pérez-Pariente, J., 2001. A new property of MCM-41: Drug delivery system. Chem. Mater. 13, 308-311.

Vallhov, H., Gabrielsson, S., Strømme, M., Scheynius, A., Garcia-Bennett, A.E., 2007. Mesoporous silica particles induce size dependent effects on human dendritic cells. Nano Lett. 7, 3576-3582.

Wang, F., Hui, H., Barnes, T.J., Barnett, C., Prestidge, C.A., 2010. Oxidized mesoporous silicon microparticles for improved oral delivery of poorly soluble drugs. Mol. Pharmaceutics 7, 227-236.

Wang, S., 2009. Ordered mesoporous materials for drug delivery. Microporous Mesoporous Mater. 117, 1-9.

Wang, T., Chai, F., Fu, Q., Zhang, L., Liu, H., Li, L., Liao, Y., Su, Z., Wang, C., Duan, B., Ren, D., 2011. Uniform hollow mesoporous silica nanocages for drug delivery in vitro and in vivo for liver cancer therapy. J. Mater. Chem. 21, 5299-5306.

Vasconcelos, T., Sarmento, B., Costa, P., 2007. Solid dispersions as strategy to improve oral bioavailability of poor water soluble drugs. Drug Discov. Today 12, 1068-1075.

Watanabe, T., Hasegawa, S., Wakiyama, N., Kusai, A., Senna, M., 2003. Comparison between polyvinylpyrrolidone and silica nanoparticles as carriers for indomethacin in a solid state dispersion. Int. J. Pharm. 250, 283-286.

Watanabe, T., Wakiyama, N., Usui, F., Ikeda, M., Isobe, T., Senna, M., 2001. Stability of amorphous indomethacin compounded with silica. Int. J. Pharm. 226, 81-91.

Verreck, G., Chun, I., Peeters, J., Rosenblatt, J., Brewster, M.E., 2003. Preparation and characterization of nanofibers containing amorphous drug dispersions generated by electrostatic spinning. Pharm. Res. 20, 810-817.

Verreck, G., Decorte, A., Heymans, K., Adriaensen, J., Cleeren, D., Jacobs, A., Liu, D., Tomasko, D., Arien, A., Peeters, J., Rombaut, P., Van den Mooter, G., Brewster, M.E., 2005. The effect of pressurized carbon dioxide as a temporary plasticizer and foaming agent on the hot stage extrusion process and extrudate properties of solid dispersions of itraconazole with PVP-VA 64. Eur. J. Pharm. Sci. 26, 349-358.

Vervaet, C., Remon, J.P., 2010. Melt granulation. In: Handbook of pharmaceutical granulation technology. Informa Healthcare, New York, NY, pp. 435-448.

Vishweshwar, P., McMahon, J.A., Bis, J.A., Zaworotko, M.J., 2006. Pharmaceutical co-crystals. J. Pharm. Sci. 95, 499-516.

Won, C.W., Nersisyan, H.H., Shin, C.Y., Lee, J.H., 2009. Porous silicon microparticles synthesis by solid flame technique. Microporous Mesoporous Mater. 126, 166-170.

Wu, C.-Y., Benet, L. Z., 2005. Predicting drug disposition via application of BCS: transport/absorption/elimination interplay and development of a biopharmaceutics drug disposition classification system. Pharm. Res. 22, 11-23.

Wu, S.-H., Lin, Y.-S., Hung, Y., Chou, Y.-H., Hsu, Y.-H., Chang, C., Mou, C.-Y., 2008. Multifunctional mesoporous silica nanoparticles for intracellular labeling and animal magnetic resonance imaging studies. ChemBioChem. 9, 53-57.

Xu, W., Gao, Q., Xu, Y., Wu, D., Sun, Y., 2009. pH-Controlled drug release from mesoporous silica tablets coated with hydroxypropyl methylcellulose phthalate. Mater. Res. Bull. 44, 606-612.

Yang, D., Kulkarni, R., Behme, R.J., Kotiyan, P.N., 2007. Effect of the melt granulation technique on the dissolution characteristics of griseofulvin. Int. J. Pharm. 329, 72-80.

Yang, K.Y., Glemza, R., Jarowski, C.I., 1979. Effects of amorphous silicon dioxides on drug dissolution. J. Pharm. Sci. 68, 560-565.

Yang, Q., Wang, S., Fan, P., Wang, L., Di, Y., Lin, K., Xiao, F.-S., 2005. pH-Responsive carrier system based on carboxylic acid modified mesoporous silica and polyelectrolyte for drug delivery. Chem. Mater. 17, 5999-6003.

Yaroshevsky, A.A., 2006. Abundances of chemical elements in the Earth's crust. Geochem. Int. 44, 48-55.

Yonemochi, E., Kitahara, S., Maeda, S., Yamamura, S., Oguchi, T., Yamamoto, K., 1999. Physicochemical properties of amorphous clarithromycin obtained by grinding and spray drying. Eur. J. Pharm. Sci. 7, 331-338.

Yu, D.-G., Branford-White, C., Shen, X.-X., Zhang, X.-F., Zhu, L.-M., 2010. Solid dispersions of ketoprofen in drug-loaded electrospun nanofibers. J. Dispersion Sci. Technol. 31, 902-908.

Yu, D.-G., Shen, X.-X., Branford-White, C., White, K., Zhu, L.-M., Bligh, S.W.A., 2009a. Oral fast-dissolving drug delivery membranes prepared from electrospun polyvinylpyrrolidone ultrafine fibers. Nanotechnology 20, 1-9.

Yu, D.-G., Zhu, L.-M., White, K., Branford-White, C., 2009b. Electrospun nanofiber-based drug delivery systems. Health 1, 67-75.

Yu, L., 2001. Amorphous pharmaceutical solids: preparation, characterization and stabilization. Adv. Drug Delivery Rev. 48, 27–42.

Zhang, Y., Zhi, Z., Jiang, T., Zhang, J., Wang, Z., Wang, S., 2010. Spherical mesoporous silica nanoparticles for loading and release of the poorly water-soluble drug telmisartan. J. Controlled Release 145, 257-263.

Zhao, D., Feng, J., Huo, Q., Melosh, N., Fredrickson, G.H., Chmelka, B.F., Stucky, G.D., 1998a. Triblock copolymer syntheses of mesoporous silica with periodic 50 to 300 Angstrom pores. Science 279, 548-552.

Zhao, D., Huo, Q., Feng, J., Chmelka, B.F., Stucky, G.D., 1998b. Nonionic triblock and star diblock copolymer and oligomeric surfactant syntheses of highly ordered, hydrothermally stable, mesoporous silica structures. J. Am. Chem. Soc. 120, 6024-6036.

Zhao, X.S., Lu, G.Q., 1998. Modification of MCM-41 by Surface Silylation with Trimethylchlorosilane and Adsorption Study. The Journal of Physical Chemistry B 102, 1556-1561.

Zhao, X.S., Lu, G.Q., Whittaker, A.K., Millar, G.J., Zhu, H.Y., 1997. Comprehensive study of surface chemistry of MCM-41 using ^{29}Si CP/MAS NMR, FTIR, pyridine-TPD, and TGA. J. Phys. Chem. B 101, 6525-6531.

Zhao, Y., Trewyn, B.G., Slowing, I.I., Lin, V.S.-Y., 2009. Mesoporous silica nanoparticle-based double drug delivery system for glucose-responsive controlled release of insulin and cyclic AMP. J. Am. Chem. Soc. 131, 8398-8400.

Zhu, Y., Shi, J., Shen, W., Dong, X., Feng, J., Ruan, M., Li, Y., 2005. Stimuli-responsive controlled drug release from a hollow mesoporous silica sphere/polyelectrolyte multilayer core-shell structure. Angew. Chem. Int. Ed. 44, 5083-5087.

Zhuravlev, L.T., 1987. Concentration of hydroxyl groups on the surface of amorphous silicas. Langmuir 3, 316-318.

Zhuravlev, L.T., 2000. The surface chemistry of amorphous silica. Zhuravlev model. Colloids Surf., A 173, 1-38.

Zijlstra, G.S., Rijkeboer, M., Van Drooge, D.J., Sutter, M., Jiskoot, W., van de Weert, M., Hinrichs, W., Frijlink, H.W., M, van Drooge, 2007. Characterization of a cyclosporine solid dispersion for inhalation. AAPS J. 9, E190-E199.